Available online at www.sciencedirect.com
SCIENCE DIRECT®
Comput. Methods Appl. Mech. Engrg. 193 (2004) 989–1011
Computer methods in applied mechanics and engineering
www.elsevier.com/locate/cma

Reproducing kernel element method Part III: Generalized enrichment and applications

Hongsheng Lu [a], Shaofan Li [b,*], Daniel C. Simkins Jr. [b], Wing Kam Liu [a], Jian Cao [a]

[a] Department of Mechanical Engineering, Northwestern University, Evanston, IL 60208, USA
[b] Department of Civil and Environmental Engineering, University of California, Berkeley, CA 94720, USA

Received 12 May 2003; received in revised form 6 August 2003; accepted 4 December 2003

Abstract

In this part of the work, a notion of generalized enrichment is proposed to construct the global partition polynomials or to enrich global partition polynomial basis with extra terms corresponding to the higher order derivatives of primary variable. This is accomplished by either multiplying enrichment functions with the original global partition polynomials, or increasing the order of global partition polynomials in the same mesh. Without refining mesh, high order consistency in interpolation hierarchy with generalized Kronecker delta property can be straightforwardly achieved in quadrilateral and triangular mesh in 2D by the proposed scheme. Comparing with the traditional finite element methods, the construction proposed here has more flexibility and only needs minimal degrees of freedom. The optimal element with high reproducing capacity and overall minimal degrees of freedom can be constructed by the generalized enrichment procedure. Two optimal elements in two dimensional space have been constructed: T10P3I$\frac{4}{3}$ triangular element satisfies third order consistency condition with only 10 degrees of freedom, and Q15P4I$\frac{4}{3}$ quadrilateral element satisfies fourth order consistency condition with 15 degrees of freedom. The performance of interpolation hierarchy is evaluated through solving some bench-mark problems for thin (Kirchhoff) plates.

Keywords: Enrichment; Finite element methods; Meshfree method; Kirchhoff plates

1. Introduction

Constructing a globally conforming I^m/C^n, $(n, m \geqslant 1)$ (I^m denotes the interpolation fields that can interpolate the derivatives of an unknown function up to mth order, and C^n denotes the interpolation fields that have continuity up to nth order derivatives.) interpolation in an arbitrary multi-dimension domain is a challenging problem for both computational geometry, approximation theory, and computational mechanics. In the early development of finite element methods, many researchers had worked on this

* Corresponding author. Tel.: +1-510-642-5362; fax: +1-510-643-8928.
E-mail address: li@ce.berkeley.edu (S. Li).

0045-7825/$ - see front matter © 2004 Elsevier B.V. All rights reserved.
doi:10.1016/j.cma.2003.12.003

subject, e.g. [1,2,8,9,14,17–20,25]. Because "the resulting schemes have always been extremely complicated in one way or another" [24], this problem has remained to be an outstanding problem for several decades.

In the Part II of this work [27], two arbitrarily smooth, globally conforming, I^m/C^n interpolation hierarchies have been constructed based on a so-called *reproducing kernel element method* (RKEM) [34], which combines the advantages of both the finite element method [5,10,24,32,33] and the meshfree method [7,12,13,15,16,26,29,30]. The proposed hierarchical interpolant possesses the generalized Kronecker property, i.e.

$$\left.\frac{\partial^{\alpha}\Psi_I^{(\beta)}}{\partial \boldsymbol{x}^{\alpha}}\right|_{\boldsymbol{x}=\boldsymbol{x}_J} = \delta_{IJ}\delta_{\alpha\beta}, \quad |\alpha|, |\beta| = 0, 1, 2, \ldots, \leqslant m,$$

where the multi-index notation is used: $\alpha = (\alpha_1, \ldots, \alpha_d)$. The quantity $|\alpha| = \sum_{i=1}^{d} \alpha_i$ is said to be the length of α. Ψ_I^{β} is the interpolation function associated with βth order derivative of the primary variable.

To construct a globally conforming RKEM interpolation fields, the key technical procedure is how to construct the so-called global partition polynomials [27,34]. In this paper, we first use Hermite (Hermite-like) interpolations to construct the global partition polynomial for primary variable and their derivatives. For the demonstration purpose, an one dimensional $I^1/C^n/P^3$ (P^k denotes the interpolation fields that can interpolate complete kth order polynomials.) interpolant of a two node element is constructed by using FEM Hermite shape functions. The same $I^1/C^n/P^3$ interpolation field is also constructed in a 2D rectangular element with minimal 4 degrees of freedom per node.

Nevertheless, it is difficult to apply this procedure to general quadrilateral elements. This is because first the Cartesian product technique may not be applied for general parallelograms, and second in constructing RKEM shape function, the global partition polynomials of an element are also evaluated at the points outside of the element, and in general the map between a quadrilateral element and its parent element may have a singular point outside the element. To circumvent these difficulties, following in Part II of this work, the Hermite interpolant along a line segment (1D) are chosen as the primary global partition polynomial, and then interpolations for derivatives are constructed by multiplying polynomial terms. The main advantage of this approach is that it can be directly applied to arbitrary triangular mesh because it only requires high order Kronecker delta properties on nodal points. However, the polynomial reproducing capacity is limited for this method. For example, I^1/C^n interpolation for triangular element can only reproduce 2D linear polynomial exactly with 3 degree of freedom for every node, i.e. $I^1/C^n/P^1$. If higher order consistency conditions are required, extra degrees of freedom associated with high order derivatives should be added to enrich the basis of the global partition polynomials. We realized that this procedure is a special p-version enrichment, because the enrichment basis functions have the generalized Kronecker delta property.

A second way to construct globally conforming shape functions is to construct global partition of polynomials by enforcing higher order polynomial reproducing properties as shown in the Part II of this work. The globally conforming shape functions constructed based on this procedure usually have better performance and approximation properties. We have successfully constructed this family of hierarchical interpolants on both triangle elements [37] and quadrilateral elements [27,28]. Examples of globally conforming triangle elements are T9P2I1, T12P3I$\frac{4}{3}$, and T18P4I3 elements [37]; and examples of globally conforming quadrilateral elements are QI2P3I1, Q16P4I2, etc. [28]. Both of these global conforming hierarchies belong to interpolation class $I^m/C^n/P^k$, $k \geqslant m$. By comparing with construction procedure of compatible finite elements, the procedure to construct compatible RKEM shape function is much flexible and versatile.

In this paper, by using the enrichment concept, we construct two optimal globally conforming interpolants with higher consistency by enriching the derivative terms of global partition polynomials in a single node, i.e. T10P3I$\frac{4}{3}$ element and Q15P4I$\frac{4}{3}$ elements. By enriching minimal mixed derivatives associated with

selected nodes, we can obtain cubic consistency in a triangle element or the fourth order consistency in a quadrilateral element.

We would like to call it procedure as a generalized enrichment. To illustrate this concept, two examples are demonstrated: T30P3I3 element and the optimal triangle element T10P3I$\frac{4}{3}$ and optimal quadrilateral element Q15P4I$\frac{4}{3}$.

This paper is organized as follows: we first outline the basic formulation of reproducing kernel element interpolation in Section 2. We then present some derivations on how to construct higher order globally conforming interpolants in Section 3. In Section 4, several examples have been given to illustrate the concept of *generalized enrichment* and its applications on construction of global partition polynomials. That is: to increase consistency condition without refining the mesh, or adding the extra nodes. The extra degrees of freedom associated with high order derivative can be considered as enrichment terms [4,6,11,31,36] to improve the accuracy of numerical solution through increasing the consistency order or enriching the specified enrichment functions.

The proposed globally conforming interpolants are applied to solve thin plate (Kirchhoff) problems in Section 5. Because of the built-in higher order Kronecker delta properties, these type of interpolants are suitable to represent the boundary data with the high order derivatives. For both simply supported and clamped thin plates, the boundary condition can be enforced exactly at boundary nodal points. Finally, a few remarks are being made in the conclusions.

2. Reproducing kernel element interpolant

Let $\Omega \subset \mathbb{R}^d$ be an open, bounded domain with a Lipschitz continuous boundary $\Gamma = \partial\Omega$. Let there be a subdivision $\{\Omega_n\}_{n=1}^N$ of the domain $\overline{\Omega} = \Omega \cup \Gamma$, i.e.:

1. Each Ω_n is a closed set with a non-empty interior.
2. $\overline{\Omega} = \cup_{n=1}^N \Omega_n$.
3. For $m \neq n$, $\overset{\circ}{\Omega}_m \cap \overset{\circ}{\Omega}_m = \emptyset$, where $\overset{\circ}{\Omega}_m$ denotes the interior of Ω_m.

On each subdomain Ω_n, we assume that for some integer $I_n \geqslant 1$, there are linearly independent global partition polynomials $\{\psi_{n,i}\}_{i=1}^{I_n}$ and corresponding nodes $\{\boldsymbol{x}_{n,i}\}_{i=1}^{I_n} \subset \Omega_n$, such that the following *reproducing property of order k* holds:

$$\sum_{i=1}^{I_n} \psi_{n,i}(\boldsymbol{x})\boldsymbol{x}_{n,i}^{\gamma} = \boldsymbol{x}^{\gamma} \quad \forall \gamma : |\gamma| \leqslant k, \ \ \forall \boldsymbol{x} \in \overline{\Omega}. \tag{2.1}$$

It should be noted that $\psi_{n,i} \in C^{\infty}(\Omega)$, $i = 1, \ldots, I_n$.

It is straightforward to construct the so-called global partition polynomials in one dimensional case. However, for multi-dimension domains, the construction is not trivial. For instance, it is difficult to construct this kind of basis function for arbitrary quadrilateral element because the mapping between quadrilateral element and parent element for evaluation points outside of element may not be exist. Fortunately, there is no difficult for the mapping if area coordinates of triangle are used to construct the global partition polynomials for triangular elements as long as the triangle is exist. On the other hand, global partition polynomials can be properly chosen such that desirable properties of approximation, for instance, higher order of consistency, minimal degree of freedom, and generalized Kronecker delta property, can be achieved by enriching the desirable extra terms.

In this new method, the global partition polynomials is patched over the whole domain and the compactly reproducing kernel function is used to decide which subdomain is included to evaluate the function

at the evaluation point [22,34,35]. The following (quasi-)interpolation operator on a continuous function $v \in C(\overline{\Omega})$ is proposed in [34] as:

$$\mathscr{I}v(\boldsymbol{x}) = \sum_{n=1}^{N}\left[\int_{\Omega_n} K_\rho(\boldsymbol{y}-\boldsymbol{x};\boldsymbol{x})\,\mathrm{d}\boldsymbol{y}\sum_{i=1}^{I_n}\psi_{n,i}(\boldsymbol{x})v(\boldsymbol{x}_{n,i})\right], \tag{2.2}$$

where, $K_\rho(\boldsymbol{z};\boldsymbol{x})$ is a kernel function which is nonzero only when $\|\boldsymbol{z}\| < \rho$. The positive number ρ represents the support size of the kernel function with respect to its first argument. The following kernel function is chosen in this work.

$$K_\rho(\boldsymbol{z};\boldsymbol{x}) = \frac{1}{\rho^d}\phi\left(\frac{\boldsymbol{z}}{\rho}\right)b(\boldsymbol{x}), \tag{2.3}$$

where the function ϕ is the *window function*, and has a support size ρ. The function $b(\boldsymbol{x})$ is to be determined under the condition of partition of unit,

$$\sum_{n=1}^{N}\left[\int_{\Omega_n} K_\rho(\boldsymbol{y}-\boldsymbol{x};\boldsymbol{x})\,\mathrm{d}\boldsymbol{y}\sum_{i=1}^{I_n}\psi_{n,i}(\boldsymbol{x})\right] = 1. \tag{2.4}$$

The interpolant of a continuous function $v \in C(\overline{\Omega})$ can then be rewritten as:

$$\mathscr{I}v(\boldsymbol{x}) = \sum_{n=1}^{N}\left[\int_{\Omega_n}\frac{1}{\rho^d}\phi\left(\frac{\boldsymbol{y}-\boldsymbol{x}}{\rho}\right)b(\boldsymbol{x})\,\mathrm{d}\boldsymbol{y}\sum_{i=1}^{I_n}\psi_{n,i}(\boldsymbol{x})v(\boldsymbol{x}_{n,i})\right] = \sum_{I=1}\Psi_I(x)v_I. \tag{2.5}$$

As shown in Part I, there are several distinguished property of this new method.

1. The interpolation operator $\mathscr{I}$ defined in (2.2) can maintain the reproducing property of global partition polynomials if the operator own the 0th reproducing property.
2. The smoothness of the global basis functions $\Psi_I(x)$ is solely determined by that of the kernel function, and is not limited by the smoothness of the finite elements.
3. The global basis functions $\Psi_I(x)$ of RKEM have the Kronecker delta property at the associated nodes, provided that some conditions on the support size of the kernel function are met.

3. Globally conforming $I^m/C^n/P^{m+2}$ interpolation fields

In this section, a special class of globally conforming $I^m/C^n/P^{m+2}$ interpolation fields are constructed in both one-dimensional space and two dimensional space. This construction only requires minimal degrees of freedom for each node. The essence of the construction is to use the continuous extension of FEM Hermite shape functions as the global partition polynomials to locally interpolate both primary variable and its derivatives directly. Conforming FEM Hermite interpolations can be realized in 1D and 2D with rectangular element. Two examples are shown in the following: 1D $I^1/C^n/P^3$ interpolant with 2 degrees of freedom for each node, and 2D $I^1/C^n/P^3$ in rectangular element with 4 degrees of freedom for each node.

Consider a two nodes element in 1D, $e \to [x_e, x_{e+1}]$. Let $\xi = (x - x_e)/L_e$ where $L_e = x_{e+1} - x_e$ the length of element. First we consider the global partition polynomials with only the terms associated with primary variable. The global partition polynomials are constructed from 1D conforming cubic Hermite FEM interpolations as:

$$\begin{aligned}\psi^{(0)}_{e,1}(x(\xi)) &= H^{(0)}_{e,1}(\xi) = 1 - 3\xi^2 + 2\xi^3,\\ \psi^{(0)}_{e,2}(x(\xi)) &= H^{(0)}_{e,2}(\xi) = 3\xi^2 - 2\xi^3,\end{aligned} \tag{3.1}$$

where the superscript (m) denotes the interpolant for the primary variable, or its mth order derivative.

This global partition polynomial own zeroth reproducing property and zeroth generalized Kronecker delta property, i.e.

$$\begin{aligned}&\psi_{e,1}^{(0)}(x(\xi))+\psi_{e,2}^{(0)}(x(\xi))=1,\\&\psi_{e,i}^{(0)}(x(\xi))\Big|_{x_{e,j}}=\delta_{ij},\quad \frac{\mathrm{d}}{\mathrm{d}(x)}\psi_{e,i}^{(0)}(x(\xi))\Big|_{x_{e,j}}=0.\end{aligned}\tag{3.2}$$

Assume that there are total N_p nodes in the domain. Based on Eq. (2.5) we have the following equation for 2 nodes element in 1D with one degree of freedom for each node.

$$\mathscr{I}v(x)=\sum_{e=1}^{N}\left[\int_{\Omega_e}\frac{1}{\rho}\phi\left(\frac{y-x}{\rho}\right)1^{\mathrm{T}}b_0(x)\,\mathrm{d}y\sum_{i=1}^{2}(\psi_{e,i}^{(0)}(x(\xi)))v(x_{e,i})\right]=\sum_{I=1}^{N_p}(\Psi_I^{(0)}(x)v_I).\tag{3.3}$$

From Part I of this work, we can find this global conforming interpolation has only zeroth order consistency because the global partition polynomials only owns zeroth order reproducing property.

To acquire higher order consistency property, extra terms with generalized Kronecker delta property are enriched in the global partition polynomials corresponding to the derivatives. The global partition polynomials are expressed as:

$$\begin{aligned}\psi_{e,1}^{(0)}(x(\xi))&=H_{e,1}^{(0)}(\xi)=1-3\xi^2+2\xi^3,\\\psi_{e,2}^{(0)}(x(\xi))&=H_{e,2}^{(0)}(\xi)=3\xi^2-2\xi^3,\\\psi_{e,1}^{(1)}(x(\xi))&=H_{e,1}^{(1)}(\xi)=\xi-2\xi^2+\xi^3,\\\psi_{e,2}^{(1)}(x(\xi))&=H_{e,2}^{(1)}(\xi)=-\xi^2+\xi^3.\end{aligned}\tag{3.4}$$

It is easy to show that the global partition polynomials own the third order reproducing conditions and generalized Kronecker delta property corresponding to the primary variable and its first derivative.

As Eq. (2.5) we have the following interpolation for 2 nodes element in 1D with two degree of freedom for each node.

$$\mathscr{I}v(x)=\sum_{e=1}^{N}\left[\int_{\Omega_e}\frac{1}{\rho}\phi\left(\frac{y-x}{\rho}\right)1^{\mathrm{T}}b_0(x)\,\mathrm{d}y\sum_{i=1}^{2}(\psi_{e,i}^{(0)}(x(\xi))v(x_{e,i})+\psi_{e,i}^{(1)}(x(\xi))v'(x_{e,i}))\right].\tag{3.5}$$

To maintain the reproducing property of the global partition polynomials, the zeroth reproducing conditions can be expressed as:

$$\sum_{e=1}^{N}\left[\int_{\Omega_e}\frac{1}{\rho}\phi\left(\frac{y-x}{\rho}\right)b_0(x)\,\mathrm{d}y\sum_{i=1}^{2}\psi_{e,i}^{(0)}(x(\xi))\right]=0.\tag{3.6}$$

The coefficient $b_0(x)$ can be obtained.

$$b_0(x)=\left[\sum_{e=1}^{N}\int_{\Omega_e}\frac{1}{\rho}\phi\left(\frac{y-x}{\rho}\right)\mathrm{d}y\right]^{-1}.\tag{3.7}$$

Finally Eq. (3.5) can be expressed as:

$$\begin{aligned}\mathscr{I}v(x) &= \sum_{e=1}^{N} b_0(x)\left[\int_{\Omega_e}\frac{1}{\rho}\phi\left(\frac{y-x}{\rho}\right)\mathrm{d}y\sum_{i=1}^{2}\left(\psi_{e,i}^{(0)}(x(\xi))v(x_{e,i})+\psi_{e,i}^{(1)}(x(\xi))v'(x_{e,i})\right)\right]\\ &= \sum_{I=1}^{N_p}\left(\Psi_I^{(0)}(x)v_I+\Psi_I'(x)v_I'\right),\end{aligned}$$

where $\Psi_I^{(0)}(x)$ and $\Psi_I^{(1)}(x)$ are the global basis functions associated with node I with respect to primary variable and its first derivative.

The following we will examine that the global basis functions $\Psi_I^{(0)}(x)$ and $\Psi_I^{(1)}(x)$ own the property of globally conforming $I^1/C^n/P^3$ interpolation, i.e. can interpolate the first derivative of unknown smoothing function, has the continuity up to its nth order derivative and can reproduce third order polynomials. The smoothness of the global basis function is dependent on the kernel function. It is no doubt that we can construct a C^n kernel function.

As shown in Part I, the global basis functions of RKEM have the Kronecker delta property at the associated nodes, provided that some conditions on the support size of the kernel function are met. In this case, the support size should be less than element length for uniform discretization.

For simplicity, we assume there is a node mapping between the local number in the element and the global number in the whole domain for node I as shown in Fig. 1 $x_I \leftrightarrow x_{e,2} \leftrightarrow x_{e+1,1}$. When the support size is less than the element length for uniform discretization, the global basis functions $\Psi_I^{(0)}$ and $\Psi_I^{(1)}(x)$ near the node I itself with two elements e and $e+1$ can be explicitly expressed as followings from Eq. (3.5)

$$\Psi_I^{(0)}(x) = \int_{\Omega_e}\frac{1}{\rho}\phi\left(\frac{y-x}{\rho}\right)b_0(x)\,\mathrm{d}y\psi_{e,2}^{(0)}(x(\xi)) + \int_{\Omega_{e+1}}\frac{1}{\rho}\phi\left(\frac{y-x}{\rho}\right)b_0(x)\,\mathrm{d}y\psi_{e+1,1}^{(0)}(x(\xi)), \tag{3.8}$$

$$\Psi_I^{(1)}(x) = \int_{\Omega_e}\frac{1}{\rho}\phi\left(\frac{y-x}{\rho}\right)b_0(x)\,\mathrm{d}y\psi_{e,2}^{(1)}(x(\xi)) + \int_{\Omega_{e+1}}\frac{1}{\rho}\phi\left(\frac{y-x}{\rho}\right)b_0(x)\,\mathrm{d}y\psi_{e+1,1}^{(1)}(x(\xi)), \tag{3.9}$$

where $b_0(x)$ is given as (3.7). From Eq. (3.7) with only two elements e and $e+1$, we can find

$$\int_{\Omega_e}\frac{1}{\rho}\phi\left(\frac{y-x}{\rho}\right)b_0(x)\,\mathrm{d}y\bigg|_{x=x_I} + \int_{\Omega_{e+1}}\frac{1}{\rho}\phi\left(\frac{y-x}{\rho}\right)b_0(x)\,\mathrm{d}y\bigg|_{x=x_I} = 1.0, \tag{3.10}$$

$$\frac{\mathrm{d}}{\mathrm{d}x}\left[\int_{\Omega_e}\frac{1}{\rho}\phi\left(\frac{y-x}{\rho}\right)b_0(x)\,\mathrm{d}y\right]\bigg|_{x=x_I} + \frac{\mathrm{d}}{\mathrm{d}x}\left[\int_{\Omega_{e+1}}\frac{1}{\rho}\phi\left(\frac{y-x}{\rho}\right)b_0(x)\,\mathrm{d}y\right]\bigg|_{x=x_I} = 0. \tag{3.11}$$

Based on Eq. (3.10), it is easy to show that $\Psi_I^{(0)}(x)$ has the Kronecker delta property, $\Psi_I^{(0)}(x_J) = \delta_{IJ}$, as $\psi_{e,2}^{(0)}(x(\xi))$ and $\psi_{e+1,1}^{(0)}(x(\xi))$ have the Kronecker delta property. For the derivative of $\Psi_I^{(0)}(x)$,

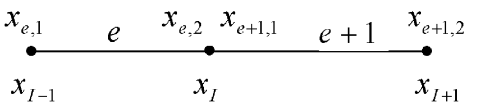

Fig. 1. Global nodal number and local nodal number.

$$\frac{\mathrm{d}}{\mathrm{d}x}\Psi_I^{(0)}(x) = \frac{\mathrm{d}}{\mathrm{d}x}\left[\int_{\Omega_e}\frac{1}{\rho}\phi\left(\frac{y-x}{\rho}\right)b_0(x)\,\mathrm{d}y\right]\psi_{e,2}^{(0)}(x(\xi)) + \int_{\Omega_e}\frac{1}{\rho}\phi\left(\frac{y-x}{\rho}\right)b_0(x)\,\mathrm{d}y\frac{\mathrm{d}}{\mathrm{d}x}\psi_{e,2}^{(0)}(x(\xi)) + \frac{\mathrm{d}}{\mathrm{d}x}\left[\int_{\Omega_{e+1}}\frac{1}{\rho}\phi\left(\frac{y-x}{\rho}\right)b_0(x)\,\mathrm{d}y\right]\psi_{e+1,1}^{(0)}(x(\xi)) + \int_{\Omega_{e+1}}\frac{1}{\rho}\phi\left(\frac{y-x}{\rho}\right)b_0(x)\,\mathrm{d}y\frac{\mathrm{d}}{\mathrm{d}x}\phi_{e+1,1}^{(0)}(x(\xi)). \tag{3.12}$$

Since the global partition polynomials $\psi_{e,2}^{(0)}(x(\xi))$ and $\psi_{e+1,1}^{(0)}(x(\xi))$ have Kronecker delta property in functions themselves and the annihilation property in their derivatives, i.e.

$$\psi_{e,2}^{(0)}(x(\xi))\Big|_{x=x_I} = 1, \quad \psi_{e+1,1}^{(0)}(x(\xi))\Big|_{x=x_I} = 0, \tag{3.13}$$

$$\frac{\mathrm{d}}{\mathrm{d}x}\psi_{e,2}^{(0)}(x(\xi))\Big|_{x=x_I} = 0, \quad \frac{\mathrm{d}}{\mathrm{d}x}\psi_{e+1,1}^{(0)}(x(\xi))\Big|_{x=x_I} = 0. \tag{3.14}$$

The derivative of $\psi_I^{(0)}(x)$ at node itself can be expressed as:

$$\frac{\mathrm{d}}{\mathrm{d}x}\Psi_I^{(0)}(x)\Big|_{(x=x_I)} = \frac{\mathrm{d}}{\mathrm{d}x}\left[\int_{\Omega_e}\frac{1}{\rho}\phi\left(\frac{y-x}{\rho}\right)b_0(x)\,\mathrm{d}y\right]\psi_{e,2}^{(0)}(x(\xi))\Big|_{x=x_I} + \frac{\mathrm{d}}{\mathrm{d}x}\left[\int_{\Omega_{e+1}}\frac{1}{\rho}\phi\left(\frac{y-x}{\rho}\right)b_0(x)\,\mathrm{d}y\right]\psi_{e+1,1}^{(0)}(x(\xi))\Big|_{x=x_I}. \tag{3.15}$$

The derivative of $\Psi_I^{(0)}(x)$ owns the annihilation property in its derivative due to Eq. (3.11). Similarly, we can show $\Psi_I^{(1)}(x)$ own the annihilation property in functions themselves and have the Kronecker delta property in their derivatives.

The global partition polynomials (conforming Hermite FEM interpolations) can reproduce any third order polynomial, and the global conforming interpolation functions $\Psi_I^{(0)}(x)$ and $\Psi_I^{(1)}(x)$ maintain this reproducing property because the zeroth reproducing condition is satisfied in the obtaining of the coefficient $b_0(x)$. It is straightforward to extend $I^1/C^n/P^3$ to high order interpolations in 1D.

Similar procedure can be applied in 2D as long as the global partition polynomials can be found. For rectangular element, the global partition polynomials can be constructed by multiplying two 1D Hermite interpolations. Consider a rectangular element in 2D as Fig. 2(a). Let $\xi = (x - x_{e,2})/L_{ex}$, $\eta = (y - y_{e,4})/L_{ey}$

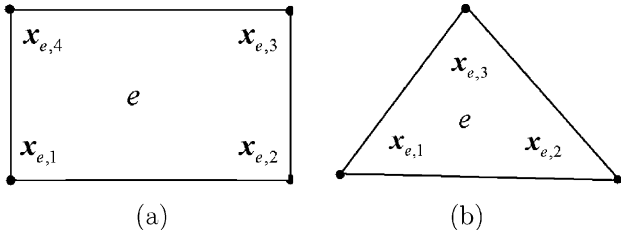

Fig. 2. 2D elements. (a) 2D rectangular element, (b) 2D triangular element.

where $L_{ex} = x_{e,2} - x_{e,1}$, $L_{ey} = y_{e,4} - y_{e,1}$. The global partition polynomials are constructed based on the conforming Hermite FEM interpolation as.

$$\begin{aligned}
&\psi_{e,1}^{(0,0)}(\boldsymbol{x}(\xi,\eta)) = H_1^{(0)}(\xi)H_1^{(0)}(\eta), \quad \psi_{e,1}^{(1,0)}(\boldsymbol{x}(\xi,\eta)) = H_1^{(1)}(\xi)H_1^{(0)}(\eta),\\
&\psi_{e,1}^{(0,1)}(\boldsymbol{x}(\xi,\eta)) = H_1^{(0)}(\xi)H_1^{(1)}(\eta), \quad \psi_{e,1}^{(1,1)}(\boldsymbol{x}(\xi,\eta)) = H_1^{(1)}(\xi)H_1^{(1)}(\eta),\\
&\psi_{e,2}^{(0,0)}(\boldsymbol{x}(\xi,\eta)) = H_2^{(0)}(\xi)H_1^{(0)}(\eta), \quad \psi_{e,2}^{(1,0)}(\boldsymbol{x}(\xi,\eta)) = H_2^{(1)}(\xi)H_1^{(0)}(\eta),\\
&\psi_{e,2}^{(0,1)}(\boldsymbol{x}(\xi,\eta)) = H_2^{(0)}(\xi)H_1^{(1)}(\eta), \quad \psi_{e,2}^{(1,1)}(\boldsymbol{x}(\xi,\eta)) = H_2^{(1)}(\xi)H_1^{(1)}(\eta),\\
&\psi_{e,3}^{(0,0)}(\boldsymbol{x}(\xi,\eta)) = H_2^{(0)}(\xi)H_2^{(0)}(\eta), \quad \psi_{e,3}^{(1,0)}(\boldsymbol{x}(\xi,\eta)) = H_2^{(1)}(\xi)H_2^{(0)}(\eta),\\
&\psi_{e,3}^{(0,1)}(\boldsymbol{x}(\xi,\eta)) = H_2^{(0)}(\xi)H_2^{(1)}(\eta), \quad \psi_{e,3}^{(1,1)}(\boldsymbol{x}(\xi,\eta)) = H_2^{(1)}(\xi)H_2^{(1)}(\eta),\\
&\psi_{e,4}^{(0,0)}(\boldsymbol{x}(\xi,\eta)) = H_1^{(0)}(\xi)H_2^{(0)}(\eta), \quad \psi_{e,4}^{(1,0)}(\boldsymbol{x}(\xi,\eta)) = H_1^{(1)}(\xi)H_2^{(0)}(\eta),\\
&\psi_{e,4}^{(0,1)}(\boldsymbol{x}(\xi,\eta)) = H_1^{(0)}(\xi)H_2^{(1)}(\eta), \quad \psi_{e,4}^{(1,1)}(\boldsymbol{x}(\xi,\eta)) = H_1^{(1)}(\xi)H_2^{(1)}(\eta),
\end{aligned} \tag{3.16}$$

where

$$\begin{aligned}
&H_{e,1}^{(0)}(\xi) = 1 - 3\xi^2 + 2\xi^3, \qquad H_{e,1}^{(0)}(\eta) = 1 - 3\eta^2 + 2\eta^3,\\
&H_{e,2}^{(0)}(\xi) = 3\xi^2 - 2\xi^3, \qquad H_{e,2}^{(0)}(\eta) = 3\eta^2 - 2\eta^3,\\
&H_{e,1}^{(1)}(\xi) = \xi - 2\xi^2 + \xi^3, \qquad H_{e,1}^{(1)}(\eta) = \eta - 2\eta^2 + \eta^3,\\
&H_{e,2}^{(1)}(\xi) = -\xi^2 + \xi^3, \qquad H_{e,2}^{(1)}(\eta) = -\eta^2 + \eta^3.
\end{aligned} \tag{3.17}$$

If we consider both the zeroth order Hermite interpolant and the higher order Hermite interpolations, we have the following operator for rectangular element in 2D with 4 degrees of freedom for each node.

$$\begin{aligned}
\mathscr{I}v(\boldsymbol{x}) &= \sum_{e=1}^{N}\left[\int_{\Omega_e}\frac{1}{\rho^2}\phi\left(\frac{\boldsymbol{y}-\boldsymbol{x}}{\rho}\right)1^{\mathrm{T}}b_0(\boldsymbol{x})\,\mathrm{d}\boldsymbol{y}\sum_{i=1}^{4}(\psi_{e,i}^{(0,0)}(\boldsymbol{x}(\xi,\eta))v^{(0,0)}(\boldsymbol{x}_{e,i})\right.\\
&\quad\left.+\psi_{e,i}^{(1,0)}(\boldsymbol{x}(\xi,\eta))v^{(1,0)}(\boldsymbol{x}_{e,i})+\psi_{e,i}^{(0,1)}(\boldsymbol{x}(\xi,\eta))v^{(0,1)}(\boldsymbol{x}_{e,i})+\psi_{e,i}^{(1,1)}(\boldsymbol{x}(\xi,\eta))v^{(1,1)}(\boldsymbol{x}_{e,i}))\right]\\
&= \sum_{I=1}^{N_p}(\Psi_I^{(0,0)}(\boldsymbol{x}(\xi,\eta))v_I + \Psi_I^{(1,0)}(\boldsymbol{x}(\xi,\eta))v_I^{(1,0)}) + (\Psi_I^{(1,1)}(\boldsymbol{x}(\xi,\eta))v_I^{(1,1)}) + (\Psi_I^{(0,1)}(\boldsymbol{x}(\xi,\eta))v_I^{(0,1)}).
\end{aligned} \tag{3.18}$$

It can be shown that the globally conforming interpolations from (3.18) can interpolate the first derivative of unknown smoothing function, has the continuity up to its nth order derivative and can reproduce third order polynomials, i.e. is one of $I^1/C^n/P^3$ interpolation in 2D.

The global basis functions of RKEM can maintain the property of basis function with only the zeroth reproducing condition and obtain conforming solution in derivatives as well. The later property will show in the next section to construct the global conforming interpolation on domain discretization with arbitrary triangular elements.

4. Compatible $I^m/C^n/P^k(k \geqslant m)$ elements in arbitrary mesh

The triangle is the most attractive element in FEM because it can be used to discretize arbitrary domains with irregular boundaries. There are a few compatible element constructed in two-dimension, e.g. Argyris element [1], Bell's element [3] and Hall's element [21], but they usually require adding extra degrees of

freedom on either nodal points or along the boundary or in the interior of the element, and the procedure cannot be extended to 3D. In this section, we will construct a globally conforming interpolation with higher order consistency and higher Kronecker delta property for triangular and quadrilateral meshes. Optimal triangular element T10P3I$\frac{4}{3}$, and optimal quadrilateral elements Q15P4I$\frac{4}{3}$ and Q6P2I$\frac{1}{3}$ are constructed by using concept of the generalized enrichment.

If a mapping between local natural coordinate ξ and global coordinate $\boldsymbol{x}$ is needed, then area coordinates of triangle are chosen such that this mapping exists for any point in the domain with arbitrary triangular elements. For each element e as Fig. 3(b), there are three nodes $(x_{e,1}, y_{e,1})$, $(x_{e,2}, y_{e,2})$ and $(x_{e,3}, y_{e,3})$, and the corresponding area coordinates for any point (x, y) in the domain can be expressed as:

$$\begin{bmatrix} \xi_{e,1} \\ \xi_{e,2} \\ \xi_{e,3} \end{bmatrix} = [\mathbf{T}]^{-1} \begin{bmatrix} 1 \\ x \\ y \end{bmatrix}, \tag{4.1}$$

$$[\mathbf{T}] = \begin{bmatrix} 1 & 1 & 1 \\ x_{e,1} & x_{e,2} & x_{e,3} \\ y_{e,1} & y_{e,2} & y_{e,3} \end{bmatrix} \quad [\mathbf{T}]^{-1} = \frac{1}{\det \mathbf{T}} \begin{bmatrix} x_{e,2}y_{e,3} - x_{e,3}y_{e,2} & y_{23} & x_{32} \\ x_{e,3}y_{e,1} - x_{e,1}y_{e,3} & y_{31} & x_{13} \\ x_{e,1}y_{e,2} - x_{e,2}y_{e,1} & y_{12} & x_{21} \end{bmatrix}, \tag{4.2}$$

where $\det \mathbf{T} = x_{21}y_{31} - x_{31}y_{21}$ and $x_{ij} = x_{e,i} - x_{e,j}$, $y_{ij} = y_{e,i} - y_{e,j}$.

4.1. The T30P3I3 element

The simple and easy understanding case is given first as a fundamental concept. Consider the global partition of polynomials in a typical triangular element as follows,

$$\begin{aligned} \psi^{(0,0)}_{e,1}(\boldsymbol{x}(\xi)) &= 1.0 - \psi^{(0,0)}_{e,2}(\boldsymbol{x}(\boldsymbol{\xi})) - \psi^{(0,0)}_{e,3}(\boldsymbol{x}(\boldsymbol{\xi})), \\ \psi^{(0,0)}_{e,2}(\boldsymbol{x}(\boldsymbol{\xi})) &= -20\xi^7_{e,2} + 70\xi^6_{e,2} - 84\xi^5_{e,2} + 35\xi^4_{e,2}, \\ \psi^{(0,0)}_{e,3}(\boldsymbol{x}(\boldsymbol{\xi})) &= -20\xi^7_{e,3} + 70\xi^6_{e,3} - 84\xi^5_{e,3} + 35\xi^4_{e,3}. \end{aligned} \tag{4.3}$$

Actually, this is the seventh order Hermite function with Kronecker delta property in the functions themselves and local annihilation property for the derivatives until third order, i.e.

$$\begin{aligned} &\psi^{(0,0)}_{e,i}(\boldsymbol{x}(\xi))\Big|_{\boldsymbol{x}_{e,j}} = \delta_{ij}, \quad i,j = 1,2,3, \\ &\frac{\partial^\beta}{\partial^\beta(\boldsymbol{x})}\psi^{(0,0)}_{e,i}(\boldsymbol{x}(\xi))\Big|_{\boldsymbol{x}_{e,j}} = 0, \quad i,j = 1,2,3 \ \ \forall|\beta| \leqslant 3. \end{aligned} \tag{4.4}$$

To maintain the reproducing condition of the basis function only the zeroth consistency is required for the operator in primary variable, Eq. (2.5) can be rewritten:

$$\mathscr{I}v(\boldsymbol{x}) = \sum_{e=1}^{N} \left[\int_{\Omega_e} \frac{1}{\rho^2} \phi\left(\frac{\boldsymbol{y} - \boldsymbol{x}}{\rho}\right) 1^{\mathrm{T}} b_0(\boldsymbol{x}) \, \mathrm{d}\boldsymbol{y} \sum_{i=1}^{3} \left(\psi^{(0,0)}_{e,i}(\boldsymbol{x}(\xi)) v^{(0,0)}(\boldsymbol{x}_{e,i}) \right) \right] = \sum_{I=1}^{N_p} \Psi^{(0,0)}_I(\boldsymbol{x}) v^{(0,0)}_I. \tag{4.5}$$

Similarly as in the previous section, it can be shown that the global conforming interpolation function $\Psi^{(0,0)}_I(\boldsymbol{x})$ associated with the primary variable has the Kronecker delta property in function itself and an annihilation property in its derivatives until to third order, provided some conditions on the support size of the kernel function are met as mentioned in Part I. Moreover the global conforming interpolation function $\Psi^{(0,0)}_I(\boldsymbol{x})$ can only reproduce the constant because the basis function $\Psi^{(0,0)}_{e,i}(\boldsymbol{x}(\xi))$, $i = 1,2,3$ has only the zeroth consistency.

To increase the order of consistency for the global conforming interpolation, extra degrees of freedom associated with the derivatives of the primary variable are added as the enrichment in the basis function such that the basis functions have the high order reproducing property. For example, we have constructed T9P2I1, T12P3I4/3, T18P2I2, and T30P3I3 elements on the triangular mesh based on global partition polynomials as denned in Eq. (4.3) (see [27,37]).

In here T30P3I3 element is constructed by enriching the global partition polynomial basis with high order derivative terms. The global partition polynomial basis with cubic reproducing property is constructed as following based on Eq. (4.3)

$$
\begin{aligned}
&\psi_{e,1}^{(0,0)}(\boldsymbol{x}(\xi)) = 1.0 - \psi_{e,2}^{(0,0)}(\boldsymbol{x}(\xi)) - \psi_{e,3}^{(0,0)}(\boldsymbol{x}(\xi)),\\
&\psi_{e,2}^{(0,0)}(\boldsymbol{x}(\xi)) = -20\xi_{e,2}^{7} + 70\xi_{e,2}^{6} - 84\xi_{e,2}^{5} + 35\xi_{e,2}^{4},\\
&\psi_{e,3}^{(0,0)}(\boldsymbol{x}(\xi)) = -20\xi_{e,3}^{7} + 70\xi_{e,3}^{6} - 84\xi_{e,3}^{5} + 35\xi_{e,3}^{4},\\
&\psi_{e,1}^{(1,0)}(\boldsymbol{x}(\xi)) = (x - x_{e,1})\psi_{e,1}^{(0,0)}(\boldsymbol{x}(\xi)) \qquad \psi_{e,1}^{(0,1)}(\boldsymbol{x}(\xi)) = (y - y_{e,1})\psi_{e,1}^{(0,0)}(\boldsymbol{x}(\xi)),\\
&\psi_{e,1}^{(2,0)}(\boldsymbol{x}(\xi)) = \frac{(x - x_{e,1})^2}{2!}\psi_{e,1}^{(0,0)}(\boldsymbol{x}(\xi)) \qquad \psi_{e,1}^{(0,2)}(\boldsymbol{x}(\xi)) = \frac{(y - y_{e,1})^2}{2!}\psi_{e,1}^{(0,0)}(\boldsymbol{x}(\xi)),\\
&\psi_{e,1}^{(1,1)}(\boldsymbol{x}(\xi)) = (x - x_{e,1})(y - y_{e,1})\psi_{e,1}^{(0,0)}(\boldsymbol{x}(\xi)) \qquad \psi_{e,1}^{(3,0)}(\boldsymbol{x}(\xi)) = \frac{(x - x_{e,1})^3}{3!}\psi_{e,1}^{(0,0)}(\boldsymbol{x}(\xi)),\\
&\psi_{e,1}^{(0,3)}(\boldsymbol{x}(\xi)) = \frac{(y - y_{e,1})^3}{3!}\psi_{e,1}^{(0,0)}(\boldsymbol{x}(\xi)),\\
&\psi_{e,1}^{(2,1)}(\boldsymbol{x}(\xi)) = \frac{(x - x_{e,1})^2(y - y_{e,1})}{2!}\psi_{e,1}^{(0,0)}(\boldsymbol{x}(\xi)),\\
&\psi_{e,1}^{(1,2)}(\boldsymbol{x}(\xi)) = \frac{(x - x_{e,1})(y - y_{e,1})^2}{2!}\psi_{e,1}^{(0,0)}(\boldsymbol{x}(\xi)) \qquad \psi_{e,2}^{(1,0)}(\boldsymbol{x}(\xi)) = (x - x_{e,2})\psi_{e,2}^{(0,0)}(\boldsymbol{x}(\xi)),\\
&\psi_{e,2}^{(0,1)}(\boldsymbol{x}(\xi)) = (y - y_{e,2})\psi_{e,2}^{(0,0)}(\boldsymbol{x}(\xi)) \qquad \psi_{e,2}^{(2,0)}(\boldsymbol{x}(\xi)) = \frac{(x - x_{e,2})^2}{2!}\psi_{e,2}^{(0,0)}(\boldsymbol{x}(\xi)),\\
&\psi_{e,2}^{(0,2)}(\boldsymbol{x}(\xi)) = \frac{(y - y_{e,2})^2}{2!}\psi_{e,2}^{(0,0)}(\boldsymbol{x}(\xi)),\\
&\psi_{e,2}^{(1,1)}(\boldsymbol{x}(\xi)) = (x - x_{e,2})(y - y_{e,2})\psi_{e,2}^{(0,0)}(\boldsymbol{x}(\xi)),\\
&\psi_{e,2}^{(3,0)}(\boldsymbol{x}(\xi)) = \frac{(x - x_{e,2})^3}{3!}\psi_{e,2}^{(0,0)}(\boldsymbol{x}(\xi)) \qquad \psi_{e,2}^{(0,3)}(\boldsymbol{x}(\xi)) = \frac{(y - y_{e,2})^3}{3!}\psi_{e,2}^{(0,0)}(\boldsymbol{x}(\xi)),\\
&\psi_{e,2}^{(2,1)}(\boldsymbol{x}(\xi)) = \frac{(x - x_{e,2})^2(y - y_{e,2})}{2!}\psi_{e,2}^{(0,0)}(\boldsymbol{x}(\xi)),\\
&\psi_{e,2}^{(1,2)}(\boldsymbol{x}(\xi)) = \frac{(x - x_{e,2})(y - y_{e,2})^2}{2!}\psi_{e,2}^{(0,0)}(\boldsymbol{x}(\xi)),\\
&\psi_{e,3}^{(1,0)}(\boldsymbol{x}(\xi)) = (x - x_{e,3})\psi_{e,3}^{(0,0)}(\boldsymbol{x}(\xi)) \qquad \psi_{e,3}^{(0,1)}(\boldsymbol{x}(\xi)) = (y - y_{e,3})\psi_{e,3}^{(0,0)}(\boldsymbol{x}(\xi)),\\
&\psi_{e,3}^{(2,0)}(\boldsymbol{x}(\xi)) = \frac{(x - x_{e,3})^2}{2!}\psi_{e,3}^{(0,0)}(\boldsymbol{x}(\xi)) \qquad \psi_{e,3}^{(0,2)}(\boldsymbol{x}(\xi)) = \frac{(y - y_{e,3})^2}{2!}\psi_{e,3}^{(0,0)}(\boldsymbol{x}(\xi)),\\
&\psi_{e,3}^{(1,1)}(\boldsymbol{x}(\xi)) = (x - x_{e,3})(y - y_{e,3})\psi_{e,3}^{(0,0)}(\boldsymbol{x}(\xi)) \qquad \psi_{e,3}^{(3,0)}(\boldsymbol{x}(\xi)) = \frac{(x - x_{e,3})^3}{3!}\psi_{e,3}^{(0,0)}(\boldsymbol{x}(\xi)),\\
&\psi_{e,3}^{(0,3)}(\boldsymbol{x}(\xi)) = \frac{(y - y_{e,3})^3}{3!}\psi_{e,3}^{(0,0)}(\boldsymbol{x}(\xi)),\\
&\psi_{e,3}^{(2,1)}(\boldsymbol{x}(\xi)) = \frac{(x - x_{e,3})^2(y - y_{e,3})}{2!}\psi_{e,3}^{(0,0)}(\boldsymbol{x}(\xi)),\\
&\psi_{e,3}^{(1,2)}(\boldsymbol{x}(\xi)) = \frac{(x - x_{e,3})(y - y_{e,3})^2}{2!}\psi_{e,3}^{(0,0)}(\boldsymbol{x}(\xi)),
\end{aligned}
\tag{4.6}
$$

i.e., the following equation is satisfied as long as the estimated function is a polynomial with the highest order is less than or equal 3.

$$\sum_{i=1}^{3}\left(\psi_{e,i}^{(0,0)}(\boldsymbol{x}(\xi))v^{(0,0)}(\boldsymbol{x}_{e,i})+\psi_{e,i}^{(1,0)}(\boldsymbol{x}(\xi))v^{(1,0)}(\boldsymbol{x}_{e,i})+\psi_{e,i}^{(0,1)}(\boldsymbol{x}(\xi))v^{(0,1)}(\boldsymbol{x}_{e,i})+\psi_{e,i}^{(1,1)}(\boldsymbol{x}(\xi))v^{(1,1)}(\boldsymbol{x}_{e,i})\right.$$
$$\left.+\psi_{e,i}^{(3,0)}(\boldsymbol{x}(\xi))v^{(3,0)}(\boldsymbol{x}_{e,i})+\psi_{e,i}^{(2,1)}(\boldsymbol{x}(\xi))v^{(2,1)}(\boldsymbol{x}_{e,i})+\psi_{e,i}^{(1,2)}(\boldsymbol{x}(\xi))v^{(1,2)}(\boldsymbol{x}_{e,i})+\psi_{e,i}^{(0,3)}(\boldsymbol{x}(\xi))v^{(0,3)}(\boldsymbol{x}_{e,i})\right)=v(\boldsymbol{x}(\xi)). \tag{4.7}$$

It is straightforward to show the third order reproducing condition of Eq. (4.7) by Talyor expansion of estimated function and its derivative at point $\boldsymbol{x}$. The fourth derivative of estimated function is zero and the other terms will cancel out based on the definition of the basis function.

With including the basis functions associated with the derivatives of primary variable, Eq. (4.5) is improved as:

$$\begin{aligned}\mathscr{I}v(\boldsymbol{x}) &= \sum_{e=1}^{N}\left[\int_{\Omega_e}\frac{1}{\rho^2}\phi\left(\frac{\boldsymbol{y}-\boldsymbol{x}}{\rho}\right)1^{\mathrm{T}}b_0(\boldsymbol{x})\,\mathrm{d}\boldsymbol{y}\sum_{i=1}^{3}(\psi_{e,i}^{(0,0)}(\boldsymbol{x}(\xi))v^{(0,0)}(\boldsymbol{x}_{e,i})+\psi_{e,i}^{(1,0)}(\boldsymbol{x}(\xi))v^{(1,0)}(\boldsymbol{x}_{e,i})\right.\\
&\quad+\psi_{e,i}^{(0,1)}(\boldsymbol{x}(\xi))v^{(0,1)}(\boldsymbol{x}_{e,i})+\psi_{e,i}^{(1,1)}(\boldsymbol{x}(\xi))v^{(1,1)}(\boldsymbol{x}_{e,i})+\psi_{e,i}^{(3,0)}(\boldsymbol{x}(\xi))v^{(3,0)}(\boldsymbol{x}_{e,i})\\
&\quad\left.+\psi_{e,i}^{(2,1)}(\boldsymbol{x}(\xi))v^{(2,1)}(\boldsymbol{x}_{e,i})+\psi_{e,i}^{(1,2)}(\boldsymbol{x}(\xi))v^{(1,2)}(\boldsymbol{x}_{e,i})+\psi_{e,i}^{(0,3)}(\boldsymbol{x}(\xi))v^{(0,3)}(\boldsymbol{x}_{e,i}))\right]\\
&= \sum_{I=1}(\Psi_I^{(0,0)}(\boldsymbol{x})v_I^{(0,0)}+\Psi_I^{(1,0)}(\boldsymbol{x})v_I^{(1,0)}+\Psi_I^{(0,1)}(\boldsymbol{x})v_I^{(0,1)}+\Psi_I^{(1,1)}(\boldsymbol{x})v_I^{(1,1)}+\Psi_I^{(2,0)}(\boldsymbol{x})v_I^{(2,0)}\\
&\quad+\Psi_I^{(0,2)}(\boldsymbol{x})v_I^{(0,2)}+\Psi_I^{(3,0)}(\boldsymbol{x})v_I^{(3,0)}+\Psi_I^{(2,1)}(\boldsymbol{x})v_I^{(2,1)}+\Psi_I^{(1,2)}(\boldsymbol{x})v_I^{(1,2)}+\Psi_I^{(0,3)}(\boldsymbol{x})v_I^{(0,3)}).\end{aligned} \tag{4.8}$$

The globally conforming interpolations defined in Eq. (4.8) own the third consistency condition because of the third order reproducing condition of basis functions and zeroth consistency condition to define the coefficient $b_0(\boldsymbol{x})$.

Now we show the globally conforming interpolation functions associated with derivatives of primary variables also own the generalized Kronecker delta property. From the definition of basis functions as Eq. (4.6) and the interpolation operator $\mathscr{I}$ as Eq. (4.8), we can find that interpolation functions $\Psi_I^{(\alpha,\beta)}(\boldsymbol{x})$, $\alpha+\beta>0$ in functions themselves and their derivatives have the annihilation property due to the multipliers including term either $(x-x_I)|_{\boldsymbol{x}=\boldsymbol{x}_I}=0$ or $(y-y_I)|_{\boldsymbol{x}=\boldsymbol{x}_I}=0$, except the derivatives of interpolation functions which are corresponding to the same order derivatives of variables; in these cases, the derivatives of interpolation functions at node points will reduce to the interpolation functions themselves which own the Kronecker delta property.

The globally conforming interpolation functions in triangular mesh are shown in Fig. 3 with total 10 degrees of freedom for node I.

4.2. The optimal T10P3I$_3^4$ and Q15P4I$_3^4$ elements

As discussed in this work of Part IV [37], the triangular element T9P2I1 as shown in Fig. 4 with three degree of freedom (primary variable and its two first derivative) for each node does not work well in solving thin plate problems. This is partly be due to the low order reproducing property. To increase the accuracy of numerical solution, we would like to increase the order of the global consistency condition of the interpolation field. To do so, we need to add the new nodal degrees of freedom to enrich the global interpolation field. For example we can construct triangular element T12P3I$_3^4$ and quadrilateral element

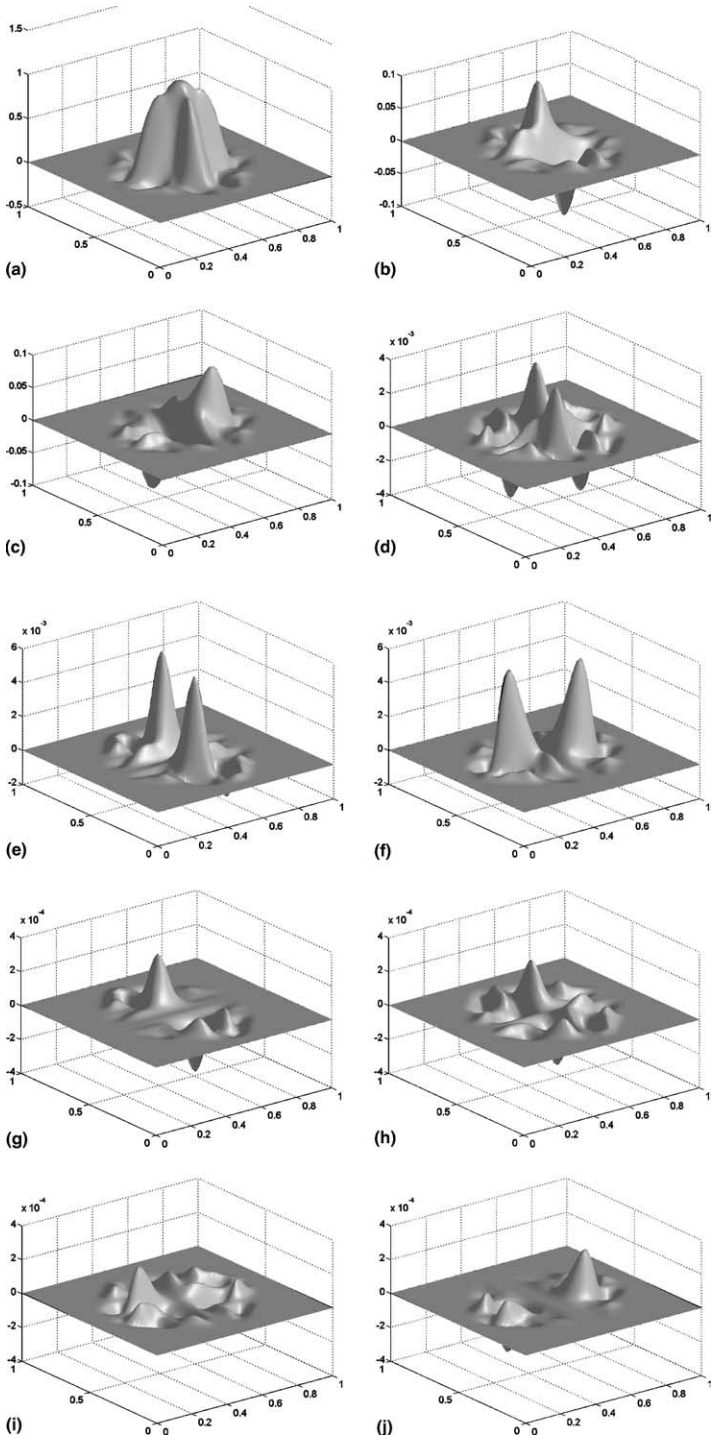

Fig. 3. Globally conforming interpolation functions. (a) $\Psi_I^{(0,0)}(\boldsymbol{x})$, (b) $\Psi_I^{(1,0)}(\boldsymbol{x})$, (c) $\Psi_I^{(0,1)}(\boldsymbol{x})$, (d) $\Psi_I^{(1,1)}(\boldsymbol{x})$, (e) $\Psi_I^{(2,0)}(\boldsymbol{x})$, (f) $\Psi_I^{(0,2)}(\boldsymbol{x})$, (g) $\Psi_I^{(3,0)}(\boldsymbol{x})$, (h) $\Psi_I^{(2,1)}(\boldsymbol{x})$, (i) $\Psi_I^{(1,2)}(\boldsymbol{x})$, (j) $\Psi_I^{(0,3)}(\boldsymbol{x})$.

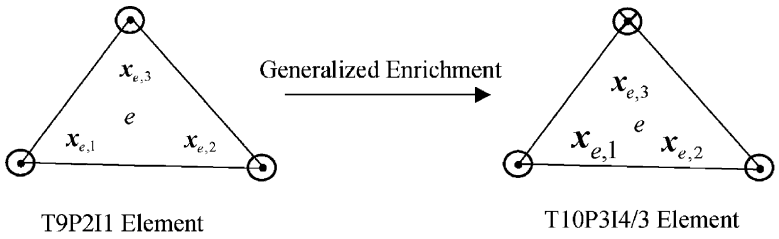

Fig. 4. Optimal triangular element $T10P3I\frac{4}{3}$.

$Q16P4I\frac{4}{3}$ by adding the degree of freedom of mixed derivatives. The degrees of freedom for each node increases from three to four. However, these elements are not optimal in the sense that they have more degrees of freedom than enough to reproduce complete cubic polynomials or the complete fourth order polynomials.

A amazing property of RKEM interpolant is that we only need to use the minimal degrees of freedom to acquire the reproducing property, i.e. we can reducing the total degrees of freedom for each element by only enriching the desirable terms at selected nodes. To demonstrate this, we have constructed triangular element $T10P3I\frac{4}{3}$ (see Fig. 4) and quadrilateral element $Q15P4I\frac{4}{3}$ (see Fig. 5), in which we use an incomplete $T10P3I\frac{4}{3}$ element to reproduce a complete cubic polynomial in a triangle mesh, and we use an incomplete $Q1P4I\frac{4}{3}$ to reproduce a complete fourth order polynomials in a quadrilateral mesh. Here the adjective, *incomplete*, refers to that we only add mixed derivative enrichment term to one node in a triangle (see Fig. 4), or we only add mixed derivative enrichment term to three nodes in a quadrilateral element, instead of adding mixed derivative enrichment terms to all the nodes.

As discussed in Part II, the global partition polynomials can be chosen as follows:

$$\sum_{i=1}^{3}\left(\psi_{e,i}^{(0,0)}v^{(0,0)}(\boldsymbol{x}_{e,i})+\psi_{e,i}^{(1,0)}v^{(1,0)}(\boldsymbol{x}_{e,i})+\psi_{e,i}^{(0,1)}v^{(0,1)}(\boldsymbol{x}_{e,i})+a_{e,i}\psi_{e,i}^{(1,1)}v^{(1,1)}(\boldsymbol{x}_{e,i})\right)$$
$$=c_1+c_2x+c_3y+c_4x^2+c_5xy+c_6y^2+c_7x^3+c_8x^2y+c_9xy^2+c_{10}y^3. \tag{4.9}$$

Besides to add the extra degree of freedom, we also can add enrichment function in the local reproduced function, the right side of the Eq. (4.9). For example, we can choose the global partition polynomials to reproduce the following local reproduced function.

$$\sum_{i=1}^{3}\left(\psi_{e,i}^{(0,0)}v^{(0,0)}(\boldsymbol{x}_{e,i})+\psi_{e,i}^{(1,0)}v^{(1,0)}(\boldsymbol{x}_{e,i})+\psi_{e,i}^{(0,1)}v^{(0,1)}(\boldsymbol{x}_{e,i})+a_{e,i}\psi_{e,i}^{(1,1)}v^{(1,1)}(\boldsymbol{x}_{e,i})\right)$$
$$=c_1+c_2x+c_3y+c_4x^2+c_5xy+c_6y^2+c_7x^3+c_8x^2(y+xy)+c_9(x+xy)y^2+c_{10}y^3, \tag{4.10}$$

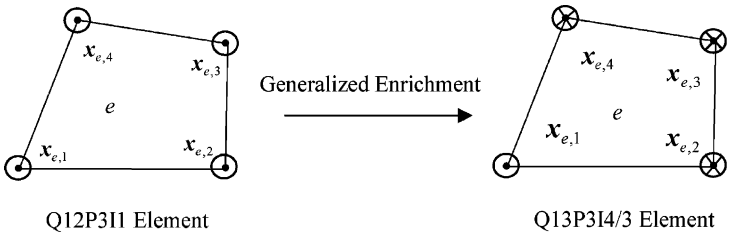

Fig. 5. Optimal quadrilateral $Q15P4I\frac{4}{3}$ element.

where $a_{e,i}$, $i = 1, 3$ are called enrichment switching coefficient with either 0 or 1. To link the nodal variables with coefficient $c's$, the following vectors $\boldsymbol{\psi}_e$, $\mathbf{v}_e$, $\mathbf{p}$, and $\mathbf{c}_e$ are defined as:

$$\begin{aligned}
\boldsymbol{\psi}_e^{\mathrm{T}}(\boldsymbol{x}) &:= \{\psi_{e,1}^{(0,0)}, \psi_{e,1}^{(1,0)}, \psi_{e,1}^{(0,1)}, a_{e,1}\psi_{e,1}^{(1,1)}, \psi_{e,2}^{(0,0)}, \psi_{e,2}^{(1,0)}, \psi_{e,2}^{(0,1)}, a_{e,2}\psi_{e,2}^{(1,1)}, \psi_{e,3}^{(0,0)}, \psi_{e,3}^{(1,0)}, \psi_{e,3}^{(0,1)}, a_{e,3}\psi_{e,3}^{(1,1)}\},\\
\mathbf{v}_e^{\mathrm{T}} &:= \{v_{e,1}^{(0,0)}, v_{e,1}^{(1,0)}, v_{e,1}^{(0,1)}, a_{e,1}v_{e,1}^{(1,1)}, v_{e,2}^{(0,0)}, v_{e,2}^{(1,0)}, v_{e,2}^{(0,1)}, a_{e,2}v_{e,2}^{(1,1)}, v_{e,3}^{(0,0)}, v_{e,3}^{(1,0)}, v_{e,3}^{(0,1)}, a_{e,3}v_{e,3}^{(1,1)}\},\\
\mathbf{p}^{\mathrm{T}}(\boldsymbol{x}) &:= \{1, x, y, x^2, xy, y^2, x^3, x^2y, xy^2, y^3\},\\
\mathbf{c}_e^{\mathrm{T}} &:= \{c_1, c_2, c_3, c_4, c_5, c_6, c_7, c_8, c_9, c_{10}\}_e.
\end{aligned} \tag{4.11}$$

Let only one mixed derivative term be enriched, i.e. one of $a_{e,i}$, $i = 1, 3$ be 1 and the others 0, then the previous vectors have the same length, and the Eq. (4.10) is rewritten for element e as:

$$\boldsymbol{\psi}_e^{\mathrm{T}}\mathbf{v}_e = \mathbf{p}^{\mathrm{T}}\mathbf{c}_e \tag{4.12}$$

To maintain the generalized Kronecker delta property of the global conforming interpolation, the nodal values are related with the coefficients $c's$ by a set of 9 simultaneous linear algebraic equations.

$$\mathbf{f}_e = \mathbf{C}_e\mathbf{c}_e, \tag{4.13}$$

where matrix $\mathbf{C}_e$ is defined by Eq. (4.14).

$$\mathbf{C}_e = \begin{vmatrix}
1 & x_1 & y_1 & x_1^2 & x_1y_1 & y_1^2 & x_1^3 & x_1^2y_1 & x_1y_1^2 & y_1^3\\
0 & 1 & 0 & 2x_1 & y_1 & 0 & 3x_1^2 & 2x_1y_1 & y_1^2 & 0\\
0 & 0 & 1 & 0 & x_1 & 2y_1 & 0 & x_1^2 & 2x_1y_1 & 3y_1^2\\
0 & 0 & 0 & 0 & a_{e,1}1 & 0 & 0 & 2a_{e,1}x_1 & 2a_{e,1}y_1 & 0\\
1 & x_2 & y_2 & x_2^2 & x_2y_2 & y_2^2 & x_2^3 & x_2^2y_2 & x_2y_2^2 & y_2^3\\
0 & 1 & 0 & 2x_2 & y_2 & 0 & 3x_2^2 & 2x_2y_2 & y_2^2 & 0\\
0 & 0 & 1 & 0 & x_2 & 2y_2 & 0 & x_2^2 & 2x_2y_2 & 3y_2^2\\
0 & 0 & 0 & 0 & a_{e,2}1 & 0 & 0 & 2a_{e,2}x_2 & 2a_{e,2}y_2 & 0\\
1 & x_3 & y_3 & x_3^2 & x_3y_3 & y_3^2 & x_3^3 & x_3^2y_3 & x_3y_3^2 & y_3^3\\
0 & 1 & 0 & 2x_3 & y_3 & 0 & 3x_3^2 & 2x_3y_3 & y_3^2 & 0\\
0 & 0 & 1 & 0 & x_3 & 2y_3 & 0 & x_3^2 & 2x_3y_3 & 3y_3^2\\
0 & 0 & 0 & 0 & a_{e,3}1 & 0 & 0 & 2a_{e,3}x_3 & 2a_{e,3}y_3 & 0
\end{vmatrix}. \tag{4.14}$$

Matrix $\mathbf{C}_e$ will reduce to 10 because only one mixed derivative is enriched. If the inverse of matrix is $\mathbf{C}_e$ well defined, then the global partition polynomials can be expressed as:

$$\boldsymbol{\psi}_e(\boldsymbol{x}) = \mathbf{C}_e^{-\mathrm{T}}\mathbf{p}(\boldsymbol{x}). \tag{4.15}$$

Plug the global partition polynomials into the Eq. (2.5), the approximation is given as:

$$\begin{aligned}
\mathscr{I}v(\boldsymbol{x}) &= \sum_{e=1}^{N}\left[\int_{\Omega_e}\frac{1}{\rho^2}\phi\left(\frac{\boldsymbol{y}-\boldsymbol{x}}{\rho}\right)1^{\mathrm{T}}b_0(\boldsymbol{x})\,\mathrm{d}\boldsymbol{y}\sum_{i=1}^{4}\left(\psi_{e,i}^{(0,0)}(\boldsymbol{x}(\xi))v^{(0,0)}(\boldsymbol{x}_{e,i}) + \psi_{e,i}^{(1,0)}(\boldsymbol{x}(\xi))v^{(1,0)}(\boldsymbol{x}_{e,i})\right.\right.\\
&\quad \left.\left. + \psi_{e,i}^{(0,1)}(\boldsymbol{x}(\xi))v^{(0,1)}(\boldsymbol{x}_{e,i}) + a_{e,i}\psi_{e,i}^{(1,1)}(\boldsymbol{x}(\xi))v^{(1,1)}(\boldsymbol{x}_{e,i})\right)\right]\\
&= \sum_{I=1}^{N_p}\left(\Psi_I^{(0,0)}(\boldsymbol{x})v_I^{(0,0)} + \Psi_I^{(1,0)}(\boldsymbol{x})v_I^{(1,0)} + \Psi_I^{(0,1)}(\boldsymbol{x})v_I^{(0,1)} + A_I\Psi_I^{(1,1)}(\boldsymbol{x})v_I^{(1,1)}\right).
\end{aligned} \tag{4.16}$$

Similarly, we can construct optimal Q15P4I$_{\frac{3}{3}}^{4}$ as shown in Fig. 5, Q13P3I$_{\frac{3}{3}}^{4}$ (adding a mixed derivative in one node), and Q6P2I$_{\frac{3}{3}}^{1}$ (adding two first order derivatives at the same one node or different two nodes)

quadrilateral elements. The Q15P4I$_5^4$ element is documented in here. The global partition polynomials can be chosen as following:

$$\begin{aligned}\sum_{i=1}^{3}\left(\psi_{e,i}^{(0,0)}v^{(0,0)}(\boldsymbol{x}_{e,i})+\psi_{e,i}^{(1,0)}v^{(1,0)}(\boldsymbol{x}_{e,i})+\psi_{e,i}^{(0,1)}v^{(0,1)}(\boldsymbol{x}_{e,i})+a_{e,i}\psi_{e,i}^{(1,1)}v^{(1,1)}(\boldsymbol{x}_{e,i})\right)\\ =c_1+c_2x+c_3y+c_4x^2+c_5xy+c_6y^2+c_7x^3+c_8x^2y+c_9xy^2+c_{10}y^3+c_{11}x^3y+c_{12}x^4\\ +c_{13}x^2y^2+c_{14}xy^3+C_{15}y^4\end{aligned} \tag{4.17}$$

and the corresponding (15×15) matrix $\mathbf{C}_e$ with choosing three mixed derivative at three nodes is defined as:

$$\mathbf{C}_e=\begin{vmatrix}
1 & x_1 & y_1 & x_1^2 & x_1y_1 & y_1^2 & x_1^3 & x_1^2y_1 & x_1y_1^2 & y_1^3 & x_1^4 & x_1^3y_1 & x_1^2y_1^2 & x_1y_1^3 & y_1^4\\
0 & 1 & 0 & 2x_1 & y_1 & 0 & 3x_1^2 & 2x_1y_1 & y_1^2 & 0 & 4x_1^3 & 3x_1^2y_1 & 2x_1y_1^2 & y_1^3 & 0\\
0 & 0 & 1 & 0 & x_1 & 2y_1 & 0 & x_1^2 & 2x_1y_1 & 3y_1^2 & 0 & x_1^3 & 2x_1^2y_1 & 3x_1y_1^2 & 4y_1^3\\
0 & 0 & 0 & 0 & a_{e,1}1 & 0 & 0 & 2a_{e,1}x_1 & 2a_{e,1}y_1 & 0 & 0 & 3a_{e,1}x_1^2 & 4a_{e,1}x_1y_1 & 3a_{e,1}y_1^2 & 0\\
1 & x_2 & y_2 & x_2^2 & x_2y_2 & y_2^2 & x_2^3 & x_2^2y_2 & x_2y_2^2 & y_2^3 & x_2^4 & x_2^3y_2 & x_2^2y_2^2 & x_2y_2^3 & y_2^4\\
0 & 1 & 0 & 2x_2 & y_2 & 0 & 3x_2^2 & 2x_2y_2 & y_2^2 & 0 & 4x_2^3 & 3x_2^2y_2 & 2x_2y_2^2 & y_2^3 & 0\\
0 & 0 & 1 & 0 & x_2 & 2y_2 & 0 & x_2^2 & 2x_2y_2 & 3y_2^2 & 0 & x_2^3 & 2x_2^2y_2 & 3x_2y_2^2 & 4y_2^3\\
0 & 0 & 0 & 0 & a_{e,2}1 & 0 & 0 & 2a_{e,2}x_2 & 2a_{e,2}y_2 & 0 & 0 & 3a_{e,2}x_2^2 & 4a_{e,2}x_2y_2 & 3a_{e,2}y_2^2 & 0\\
1 & x_3 & y_3 & x_3^2 & x_3y_3 & y_3^2 & x_3^3 & x_3^2y_3 & x_3y_3^2 & y_3^3 & x_3^4 & x_3^3y_3 & x_3^2y_3^2 & x_3y_3^3 & y_3^4\\
0 & 1 & 0 & 2x_3 & y_3 & 0 & 3x_3^2 & 2x_3y_3 & y_3^2 & 0 & 4x_3^3 & 3x_3^2y_3 & 2x_3y_3^2 & y_3^3 & 0\\
0 & 0 & 1 & 0 & x_3 & 2y_3 & 0 & x_3^2 & 2x_3y_3 & 3y_3^2 & 0 & x_3^3 & 2x_3^2y_3 & 3x_3y_3^2 & 4y_3^3\\
0 & 0 & 0 & 0 & a_{e,3}1 & 0 & 0 & 2a_{e,3}x_3 & 2a_{e,3}y_3 & 0 & 0 & 3a_{e,3}x_3^2 & 4a_{e,3}x_3y_3 & 3a_{e,3}y_3^2 & 0\\
1 & x_4 & y_4 & x_4^2 & x_4y_4 & y_4^2 & x_4^3 & x_4^2y_4 & x_4y_4^2 & y_4^3 & x_4^4 & x_4^3y_4 & x_4^2y_4^2 & x_4y_4^3 & y_4^4\\
0 & 1 & 0 & 2x_4 & y_4 & 0 & 3x_4^2 & 2x_4y_4 & y_4^2 & 0 & 4x_4^3 & 3x_4^2y_4 & 2x_4y_4^2 & y_4^3 & 0\\
0 & 0 & 1 & 0 & x_4 & 2y_4 & 0 & x_4^2 & 2x_4y_4 & 3y_4^2 & 0 & x_4^3 & 2x_4^2y_4 & 3x_4y_4^2 & 4y_3^3\\
0 & 0 & 0 & 0 & a_{e,4}1 & 0 & 0 & 2a_{e,4}x_4 & 2a_{e,4}y_4 & 0 & 0 & 3a_{e,4}x_4^2 & 4a_{e,4}x_4y_4 & 3a_{e,4}y_4^2 & 0
\end{vmatrix}, \tag{4.18}$$

and the final approximation is given as:

$$\begin{aligned}\mathscr{I}v(\boldsymbol{x})&=\sum_{e=1}^{N}\left[\int_{\Omega_e}\frac{1}{\rho^2}\phi\left(\frac{\boldsymbol{y}-\boldsymbol{x}}{\rho}\right)1^{\mathrm{T}}b_0(\boldsymbol{x})\,\mathrm{d}\boldsymbol{y}\sum_{i=1}^{4}\left(\psi_{e,i}^{(0,0)}(\boldsymbol{x}(\xi))v^{(0,0)}(\boldsymbol{x}_{e,i})+\psi_{e,i}^{(1,0)}(\boldsymbol{x}(\xi))v^{(1,0)}(\boldsymbol{x}_{e,i})\right.\right.\\ &\left.\left.+\psi_{e,i}^{(0,1)}(\boldsymbol{x}(\xi))v^{(0,1)}(\boldsymbol{x}_{e,i})+a_{e,i}\psi_{e,i}^{(1,1)}(\boldsymbol{x}(\xi))v^{(1,1)}(\boldsymbol{x}_{e,i})\right)\right]\\ &=\sum_{I=1}^{N_p}\left(\Psi_I^{(0,0)}(\boldsymbol{x})v_I^{(0,0)}+\Psi_I^{(1,0)}(\boldsymbol{x})v_I^{(1,0)}+\Psi_I^{(0,1)}(\boldsymbol{x})v_I^{(0,1)}+A_I\Psi_I^{(1,1)}(\boldsymbol{x})v_I^{(1,1)}\right).\end{aligned} \tag{4.19}$$

5. Numerical results

In this section, we report numerical results for the performance of the globally conforming interpolation $I^3/C^4/P^3$ with T30P3I3 and T12P3I3 elements in solving thin plate problems with Kirchhoff plate theory.

5.1. Equilateral triangular plate

To validate the method, an equilateral triangular thin plate under uniform load is solved first by using the proposed method. The coordinate axes are taken as shown in Fig. 6(a). In the case of a uniformly loaded with simply support the deflection of surface is given as [40]:

$$w = \frac{p}{64aD}\left[x^3 - 3y^2x - a(x^2+y^2) + \frac{4}{27}a^3\right]\left(\frac{4}{9}a^2 - x^2 - y^2\right), \tag{5.1}$$

where D is the flexural rigidity of the plate, q is external force and a is the height of the triangle plate.

Three discretizations with 9, 36, and 144 T30P3I3 elements shown in Fig. 7 are used for convergency study. Due to the generalized Kronecker delta property of globally conforming interpolation, it is easy to exactly impose the simply supported boundary conditions. Sixty four quadrature points for each triangular element are used in the Galerkin approach. The maximum deflection at center for three cases are, $1.08428070\text{E}{-}03\frac{pa^4}{D}$, $1.03376896\text{E}{-}03\frac{pa^4}{D}$, $1.02974603\text{E}{-}03\frac{pa^4}{D}$ respectively, and the exact solution is $1.02880658\text{E}{-}03\frac{pa^4}{D}$. The deflection surfaces corresponding to three models are shown in Fig. 8. The L_2 error norms in primary variable, its first and second derivatives are shown in Fig. 9 for interpolation and Galerkin solutions, respectively. The convergency rates in terms of error norms L_2, H^1 and H^2 are 3.2, 2.8, and 1.7 for Galerkin solution, respectively. They match well with the convergency rates for interpolation solution, which are 3.4, 2.4, and 1.4 in terms of error norms L_2, H^1 and H^2, respectively.

5.2. Square plate

Square plate under uniformly distributed load q with different boundary conditions is analyzed in this example. The geometry and axes coordinate of plate are illustrated in Fig. 6(b). Two cases with simply supported and clamped square plate are examined in here. For simply supported square plate, the deflection is given as [40]:

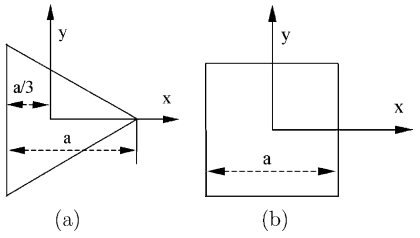

Fig. 6. Problem description for plate. (a) Triangle plate, (b) square plate.

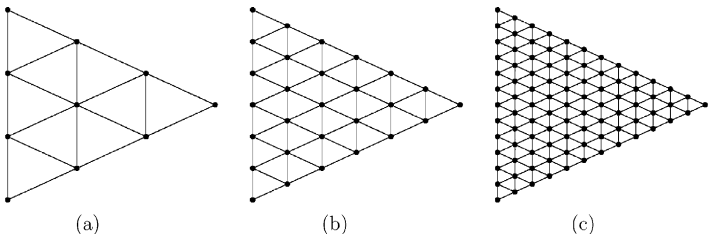

Fig. 7. Model discretizations for triangle thin plate. (a) 10 nodes, (b) 28 nodes, (c) 91 nodes.

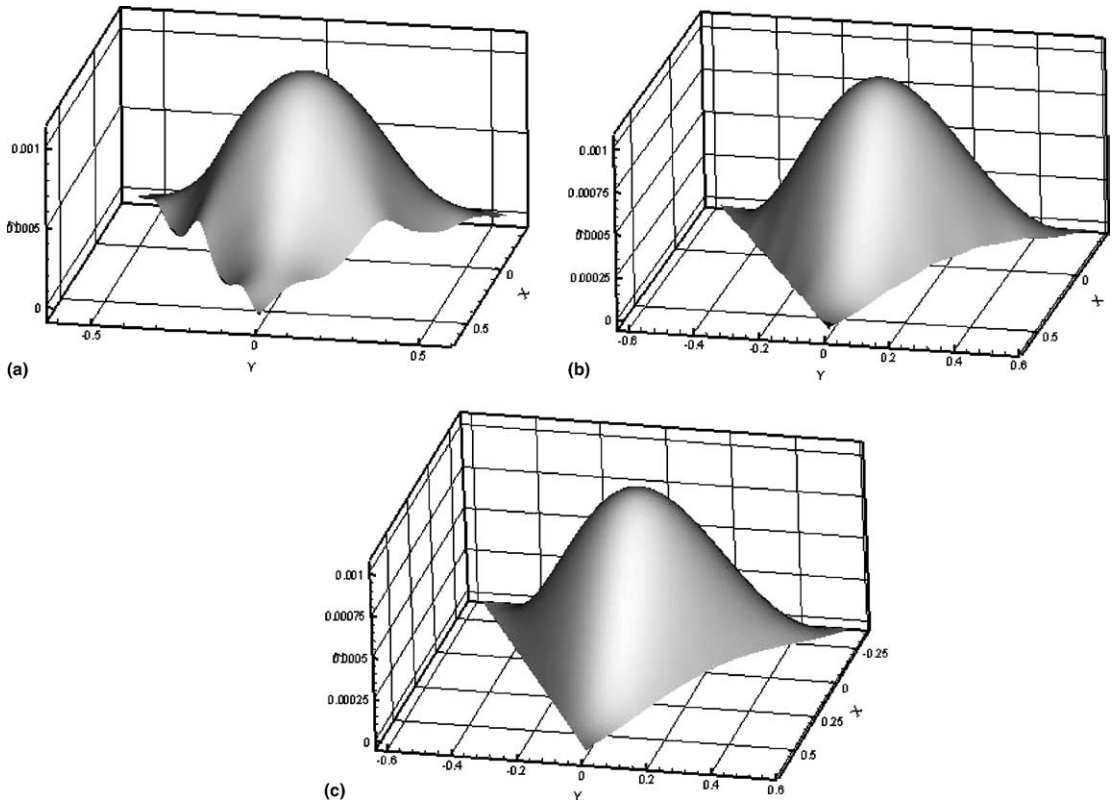

Fig. 8. Deflection for triangle plate: (a) 9 elements, (b) 36 elements (c) 144 elements.

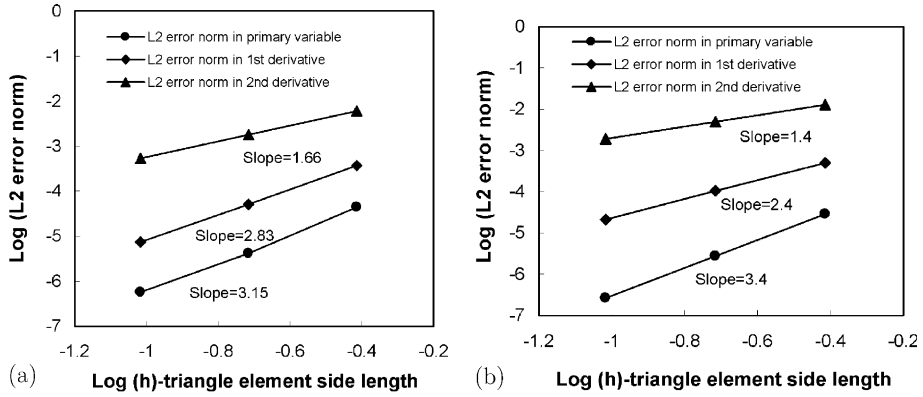

Fig. 9. Convergency rates of interpolation and Galerkin solutions: (a) L_2 error norms for a Galerkin solution; (b) L_2 error norms for interpolation solution.

$$w = \frac{4pa^4}{\pi^5 D} \sum_{m=1,3,5,\ldots}^{\infty} \frac{(-1)^{(m-1)/2}}{m^5} \cos\frac{m\pi x}{a} \left[1 - \frac{\alpha_m \tanh\alpha_m + 2}{2\cosh\alpha_m} \cosh\frac{m\pi y}{a} + \frac{1}{2\cosh\alpha_m} \frac{m\pi y}{a} \sinh\frac{m\pi y}{a}\right], \quad (5.2)$$

where $\alpha_m = m\pi/2$. 200 terms of Eq. (5.2) are used to calculate the deflections of the exact solution for comparing with the numerical solutions, and the maximum deflection at middle point is given as 4.06234741E−03$\frac{qa^4}{D}$. Three discretizations as shown in Fig. 10 with 16, 64, and 256 T30P3I3 elements, respectively, are employed to convergency test. The deflection of plate are illustrated in Fig. 11 for three models. The maximum deflections for three models are 4.14090792E−3$\frac{qa^4}{D}$, 4.05844085E−03$\frac{qa^4}{D}$, 4.06289298E−03$\frac{qa^4}{D}$, respectively. Convergency rates in terms of L_2 error norms in primary variable, the first and second derivatives are given in Fig. 12 for Galerkin and interpolation solutions. High convergency rates, with 4.37, 3.33 and 2.00 in L_2, H^1 and H^2, respectively, can be observed in Galerkin solution.

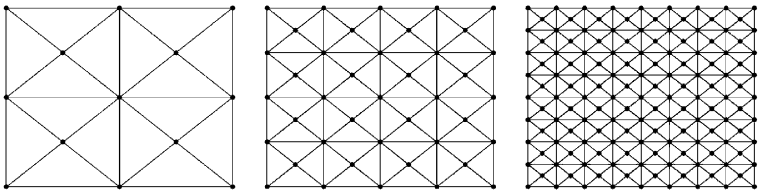

Fig. 10. Model discretizations for square thin plate. (a) 16 elements, (b) 64 elements, (c) 256 elements.

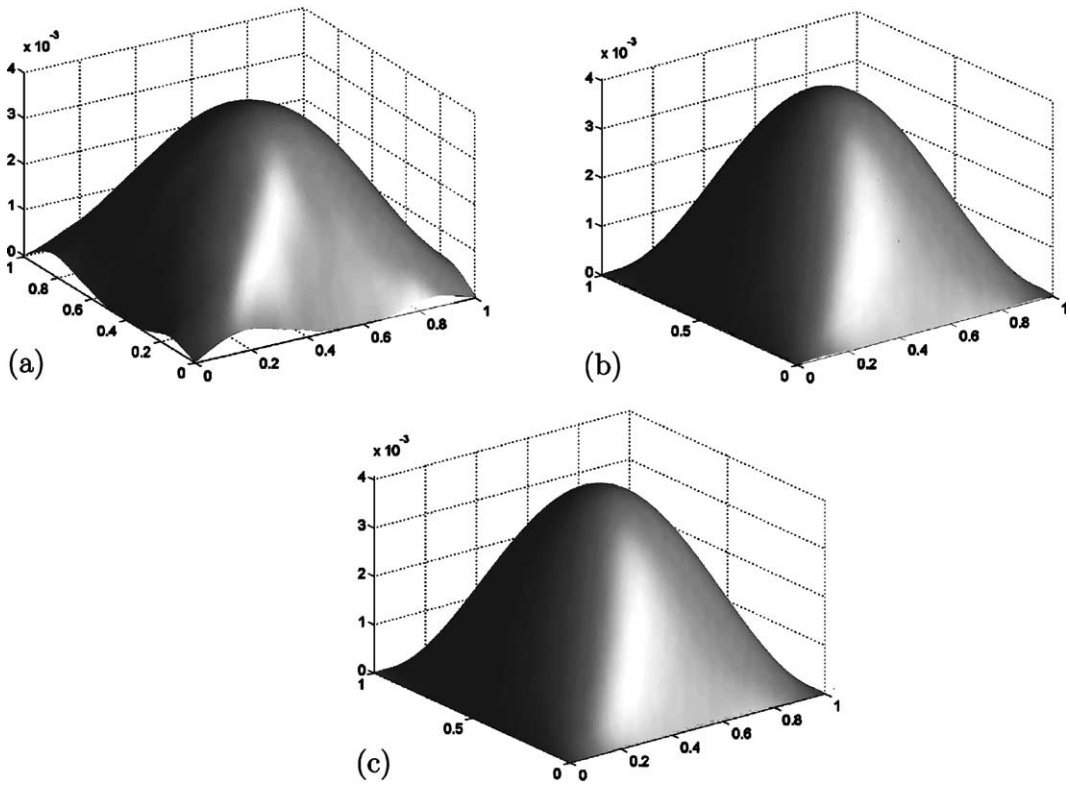

Fig. 11. Deflection for square thin plate: (a) 16 elements, (b) 64 elements (c) 256 elements.

For clamped square plate,the numerical results of T30P3I3 and T12P3I3 elements are compared. Two formulations of exact solution which have been proposed are the double cosine series [38] and Hencky's

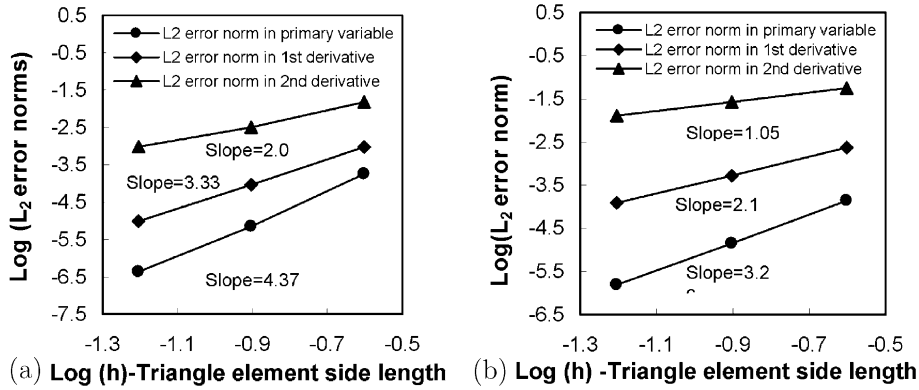

Fig. 12. Convergency rates of interpolation and Galerkin solutions: (a) L_2 error norms for a Galerkin solution; (b) L_2 error norms for interpolation solution.

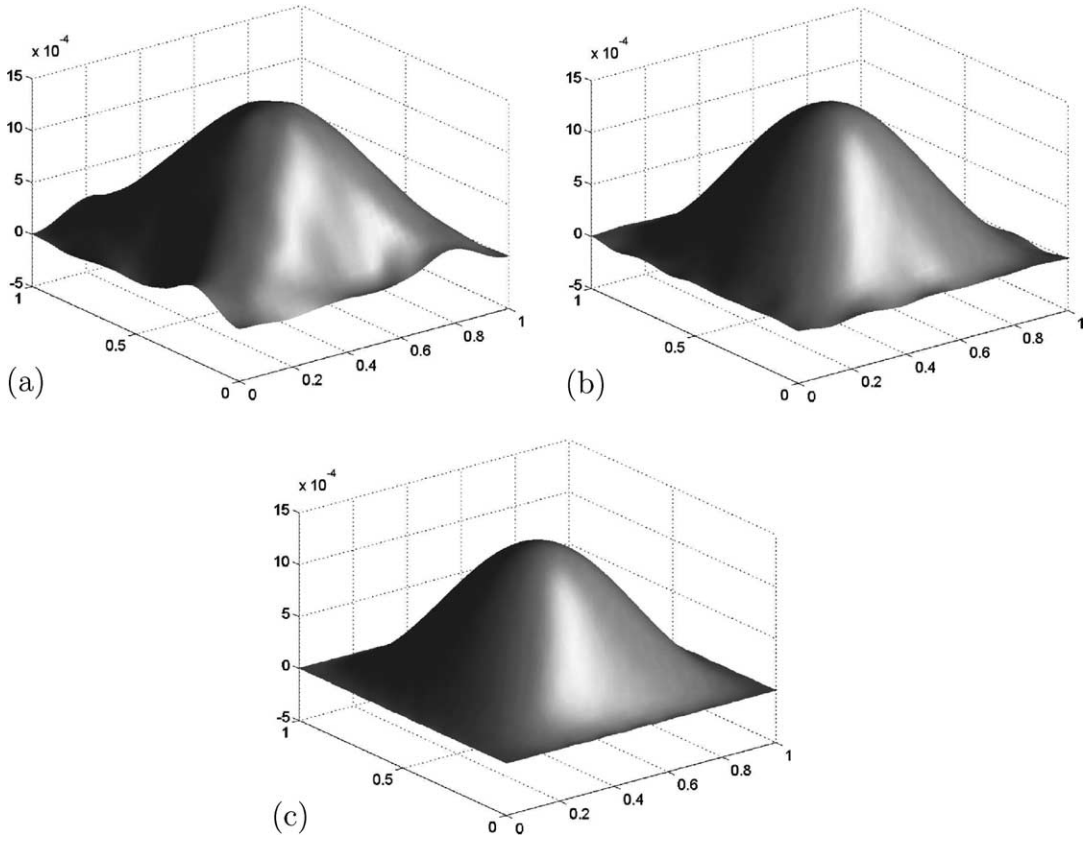

Fig. 13. Deflection for square thin plate with T30P3I3 element: (a) 16 elements, (b) 64 elements (c) 256 elements.

method [23]. In here the double cosine series with total 250×250 terms is used to approximate the exact solutions.

$$w(x,y)=\sum_{m=1}^{M}\sum_{n=1}^{N}(1-\cos 2m\pi x/a)(1-\cos 2n\pi y/a)w_{mn}. \tag{5.3}$$

The deflections of three discretzations are shown in Figs. 13 and 14 for T30P3I3 and T12P3I3 elements, respectively. For the coarse model, there is high error near the boundary partly due to high order consistency of shape function; The numerical solutions will be improved rapidly when the model becomes fine. The convergency rates of Galerkin solution with T30P3I3 element (0.8, 0.8, and 0.7) is slower than these of Galerkin solution with T12P3I4/3 element (1.9, 1.6, and 1.0) as shown in Fig. 15(a); However, for interpolation solution the convergency rates by using T30P3I3 element match with these by using T12P3I4/3 element as shown in Fig. 15(b). As given in [39], the accurate E work which defined as following is $3.891200775\text{E}{-}04\frac{D}{q^2a^4}$ for clamped square plate.

$$E=\int_A qw(x,y)\,\mathrm{d}A. \tag{5.4}$$

The convergency rate of Galerkin solution in terms of error in E work is 0.97 and 3.17 for T30P3I3 and T12P3I4/3 elements, respectively, as plotted in Fig. 16.

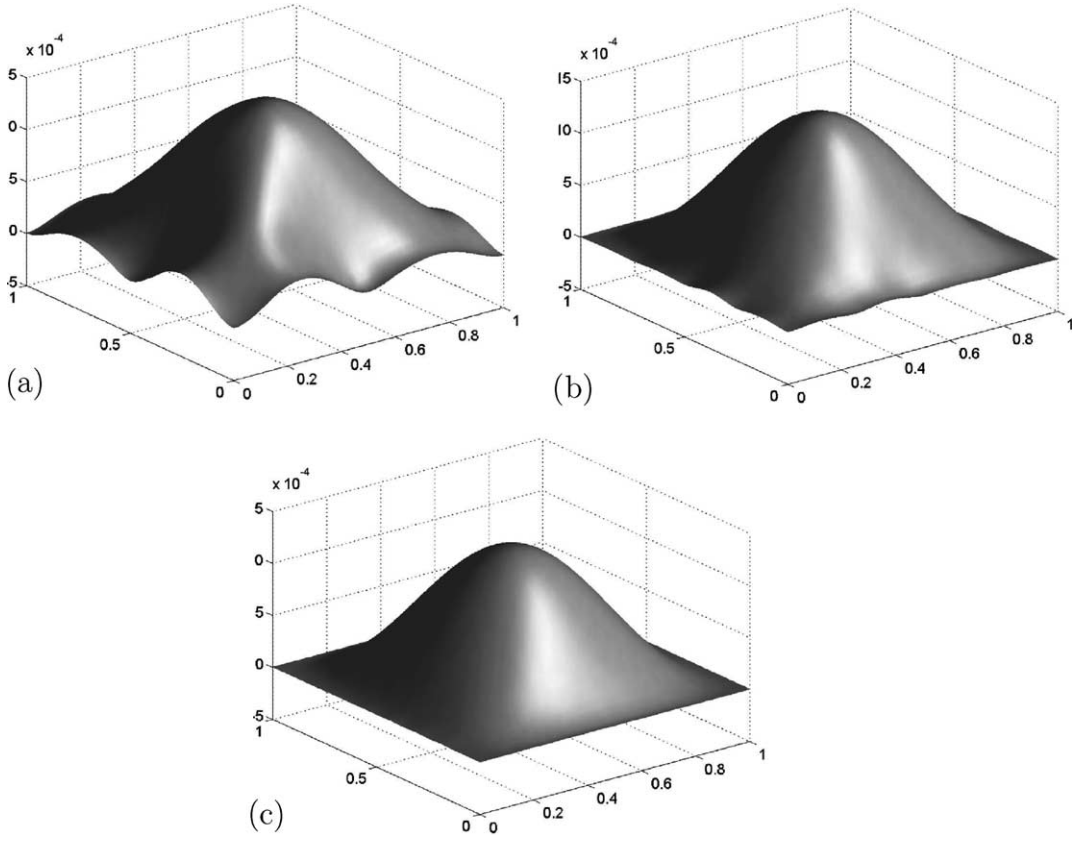

Fig. 14. Deflection for square thin plate with T12P3I4/3 element: (a) 16 elements, (b) 64 elements (c) 256 elements.

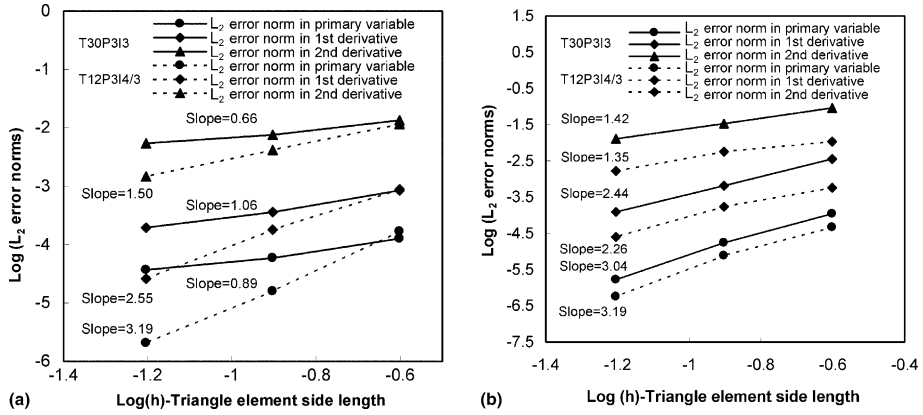

Fig. 15. Convergence rates of interpolation and Galerkin solutions: (a) L_2 error norms for a Galerkin solution; (b) L_2 error norms for interpolation solution.

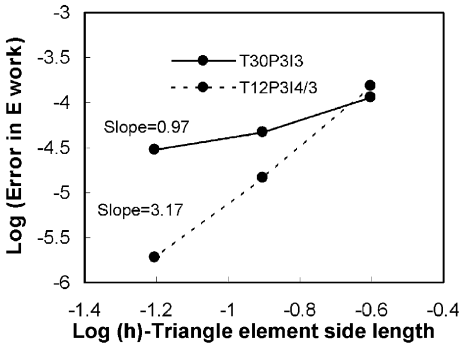

Fig. 16. Convergency rate of Galerkin solution in terms of E work.

6. Concluding remarks

In this work, we have constructed globally conforming interpolation functions $I^m/C^n/P^k$ $(k \geqslant m)$ by following a generalized enrichment procedure.

Without adding new nodes, high order consistency of interpolation hierarchy can be achieved in rectangular elements, quadrilateral elements, and triangular elements. The proposed interpolants have higher order Kronecker delta property, which is desirable especially in solving Galerkin weak formers of high order partial differential equations and in treating higher order Dirichlet boundary conditions, for example computations of Kirchhoff plates and shells. Numerical examples show the satisfactory performance of the globally conforming interpolants when they are used solving thin plate problems. A study to use these interpolants to solve Kirchhoff shell problems will be reported in a separated paper.

Acknowledgements

This work is made possible by support from NSF under the grant DMI-0115079 to Northwestern University, and CMS-0239130 to University of California (Berkeley), which are greatly appreciated.

References

[1] J.H. Argyris, I. Fried, D.W. Scharpf, The TUBA family of plate elements for the matrix displacement method, Aeronaut. Royal Aeronaut. Soc. 72 (1968) 701–709.
[2] G.P. Bazeley, Y.K. Cheung, B.M. Irons, O.C. Zienkiewicz, Triangle elements in bending: conforming and nonconforming solutions, in: Proc. 1st Conference on Matrix Methods in Structural Mechanics, Wright-Patterson, AFB, Ohio, 1965.
[3] K. Bell, A refined triangular plate bending finite element, Int. J. Numer. Methods Engrg. 1 (1969) 101–122.
[4] T. Belytschko, M. Fleming, Smoothing, enrichment and contact in the element-free Galerkin method, Comput. Struct. 71 (1999) 173–195.
[5] T. Belytschko, W.K. Liu, B. Moran, Nonlinear Finite Elements for Continua and Structures, Wiley, England, 2000.
[6] T. Belytschko, N. Moes, S. Usui, C. Parimi, Arbitrary discontinuities infinite elements, Int. J. Numer. Methods Engrg. 50 (2001) 993–1013.
[7] T. Belytschko, Y.Y. Lu, L. Gu, Element-free Galerkin methods, Int. J. Numer. Methods Engrg. 37 (1994) 229–256.
[8] G. Birkhoff, C. de Boor, Piecewise polynomial interpolation and approximation, in: H.L. Garabedian (Ed.), Approximation of Functions, Elsevier, New York, 1965.
[9] G. Birkhoff, M.H. Schultz, R.S. Varga, Piecewise Hermite interpolation in one and two variables with applications to partial differential equations, Numer. Math. 11 (1968) 232–256.
[10] S.C. Brenner, L.R. Scott, The Mathematical Theory of Finite Element Methods, Springer-Verlag, New York, 1994.
[11] J.S. Chen, W. Han, Y. You, X. Meng, A reproducing kernel method with nodal interpolation property, Int. J. Numer. Methods Engrg. 56 (2003) 935–960.
[12] J.S. Chen, C.T. Wu, S. Yoon, Y. You, A stabilized conforming nodal integration for Galerkin meshfree methods, Int. J. Numer. Methods Engrg. 50 (2001) 435–466.
[13] J.S. Chen, C. Pan, C.T. Wu, W.K. Liu, Reproducing kernel particle methods for large deformation analysis of nonlinear structures, Comput. Methods Appl. Mech. Engrg. 139 (1996) 195–229.
[14] R.W. Clough, J. Tocher, Finite element stiffness matrices for the analysis of plate bending, in: Proc. 1st Conference on Matrix Methods in Structural Mechanics, Wright-Patterson, AFB, Ohio, 1965.
[15] B. Donning, W.K. Liu, Meshless methods for shear-deformable beams and plates, Comput. Methods Appl. Mech. Engrg. 152 (1998) 47–72.
[16] C.A.M. Duarte, J.T. Oden, A hp adaptive method using clouds, Comput. Methods Appl. Mech. Engrg. 139 (1996) 237–262.
[17] I. Ergatoudis, B.M. Irons, O.C. Zienkiewicz, Curved, isoparametric, ''quadrilateral'' elements for finite element analysis, Int. J. Solids Struct. 4 (1968) 31–42.
[18] C. Felippa, R.W. Clough, The finite element in solid mechanics, in: SIAM-AMS Proceedings, vol. 2, Amer. Math. Soc, Providence, RI, 1970, pp. 210–252.
[19] de Veubeke, B. Fraeijs, Bending and stretching of plates—special models for upper and lower bounds, in: Proc. 1st Conference on Matrix Methods in Structural Mechanics, Wright-Patterson, AFB, Ohio, 1965.
[20] de Veubeke, B. Fraeijs, A conforming finite element for plate bending, Int. J. Solids Struct. 4 (1968) 95–108.
[21] C.A. Hall, Bicubic interpolation over triangles, J. Math. Mech. 19 (1969) 1–11.
[22] S. Hao, W.K. Liu, Revisit of moving particle finite element method, in: Fifth World Congress on Computational Mechanics, Vienna, Austria, 7–12 July 2002.
[23] H. Hencky, Der Spannungszustand in rechtechigen platten, Ph.D. thesis, Darmstadt, Published by R. Oldenbourg, Munich and Berlin, Germany, 1913.
[24] T.J.R. Hughes, The Finite Element Method, Prentice Hall Inc, Englewood Cliffs, NJ, 1987.
[25] B.M. Irons, A conforming quartic triangular element for plate bending, Int. J. Numer. Methods Engrg. 1 (1969) 29–45.
[26] S. Li, W.K. Liu, Meshfree and particle methods and their applications, Appl. Mech. Rev. 55 (2002) 1–34.
[27] S. Li, H. Lu, W. Han, W.K. Liu, D.C. Simkins, Reproducing kernel element, Part II. Global conforming I^m/C^n hierarchy, Comput. Meth. Appl. Mech. Engrg., in press.
[28] S. Li, D.C. Simkins Jr., H. Lu, Compatible reproducing kernel quadrilateral elements and applications, in press.
[29] W.K. Liu, Y. Chen, R.A. Uras, T.C. Chang, Generalized multiple scale reproducing kernel particle methods, Comput. Methods Appl. Mech. Engrg. 139 (1996) 91–157.
[30] W.K. Liu, S. Jun, Y.F. Zhang, Reproducing kernel particle methods, Int. J. Numer. Methods Fluids 20 (1995) 1081–1106.
[31] W.K. Liu, R.A. Uras, Y. Chen, Enrichment of the finite element method with the reproducing kernel particle method, J. Appl. Mech., ASME 64 (1997) 861–870.
[32] W.K. Liu, Y. Guo, S. Tang, T. Belytschko, A multiple-quadrature eight-node hexahedral finite element for large deformation elastoplastic analysis, Comput. Methods Appl. Mech. Engrg. 154 (1998) 69–132.
[33] W.K. Liu, Y. Zhang, M.R. Ramirez, Multiple scale finite element methods, Int. J. Numer. Methods Engrg. 32 (1991) 969–990.
[34] W.K. Liu, W. Han, H. Lu, S. Li, J. Cao, Reproducing kernel element, Part I. Theoretical formulation, Comput. Methods Appl. Mech. Engrg., in press.

[35] H. Lu, W.K. Liu, J.S. Chen, J. Cao, Consistent reproducing kernel element smoothing in progressive adaptive finite element method, Int. J. Numer. Methods Engrg., in press.
[36] H. Lu, H.S. Cheng, J. Cao, W.K. Liu, Adaptive enrichment meshfree simulation and experiment on buckling and post-buckling analysis in sheet metal forming, Comput. Methods Appl. Mech. Engrg., in press.
[37] D.C. Simkins Jr., S. Li, H. Lu, W.K. Liu, Reproducing kernel element method, Part IV. Globally conforming $C^n(n \geqslant 1)$ triangular hierarchy, Comput. Methods Appl. Mech. Engrg., in press.
[38] R. Szilard, Theory and Analysis of Plates, Prentice-Hall, Englewood Cliffs, NJ, 1974.
[39] R.L. Taylor, S. Govinfjee, Solution of clamped rectangular plate problems, Technical Report, UCB/SEMM-2002/09, University of California, Berkeley.
[40] S.P. Timoshenko, S. Woinowsky-Krieger, Theory of Plates and Shells, second ed., McGraw-Hill, New York, 1959.